AGU PUBLICATIONS

JGR

Journal of Geophysical Research: Solid Earth

RESEARCH ARTICLE
10.1002/2016JB013560

Key Points:
- Five megathrust ruptures occurred below the Mentawai Islands during the seventeenth century, the culmination of an earthquake supercycle
- As was the case for the 1797/1833 culmination, the pattern of megathrust coupling changed during the rupture sequence
- Older coral data support our characterization of Mentawai segment megathrust behavior, informing future expectations

Supporting Information:
- Supporting Information S1
- Movie S1

Correspondence to:
B. Philibosian,
bphilibosian@usgs.gov

Citation:
Philibosian, B., et al. (2017), Earthquake supercycles on the Mentawai segment of the Sunda megathrust in the seventeenth century and earlier, *J. Geophys. Res. Solid Earth*, *122*, 642–676, doi:10.1002/2016JB013560.

Received 17 SEP 2016
Accepted 12 DEC 2016
Accepted article online 15 DEC 2016
Published online 26 JAN 2017

Earthquake supercycles on the Mentawai segment of the Sunda megathrust in the seventeenth century and earlier

Belle Philibosian[1,2], Kerry Sieh[3], Jean-Philippe Avouac[1], Danny H. Natawidjaja[4], Hong-Wei Chiang[5], Chung-Che Wu[4], Chuan-Chou Shen[4], Mudrik R. Daryono[6], Hugo Perfettini[1,7], Bambang W. Suwargadi[4], Yanbin Lu[3], and Xianfeng Wang[3]

[1]Tectonics Observatory, Division of Geological and Planetary Sciences, California Institute of Technology, Pasadena, California, USA, [2]Now at U.S. Geological Survey, Menlo Park, California, USA, [3]Earth Observatory of Singapore, Nanyang Technological University, Singapore, [4]Research Center for Geotechnology, Indonesian Institute of Science (LIPI), Bandung, Indonesia, [5]High-Precision Mass Spectrometry and Environment Change Laboratory, Department of Geosciences, National Taiwan University, Taipei, Taiwan, [6]Institut Teknologi Bandung, Bandung, Indonesia, [7]Now at IRD/ISTerre, Université Joseph Fourier, Grenoble, France

Abstract Over at least the past millennium, the Mentawai segment of the Sunda megathrust has failed in sequences of closely timed events rather than in single end-to-end ruptures—each the culmination of an earthquake "supercycle." Here we synthesize the sixteenth- and seventeenth-century coral microatoll records into a chronology of interseismic and coseismic vertical deformation. We identify at least five discrete uplift events in about 1597, 1613, 1631, 1658, and 1703 that likely correspond to large megathrust ruptures. This sequence contrasts with the following supercycle culmination, which involved only two large ruptures in 1797 and 1833. Fault slip modeling suggests that together the five cascading ruptures involved failure of the entire Mentawai segment. Interseismic deformation rates also changed after the onset of the rupture sequence, as they did after the 1797 earthquake. We model this change as an altered distribution of fault coupling, presumably triggered by the ~1597 rupture. We also analyze the far less continuous microatoll record between A.D. 1 and 1500. While we cannot confidently delineate the extent of any megathrust rupture during that period, all evidence suggests that individual major ruptures involve only part of the Mentawai segment, often overlap below the central Mentawai Islands, often trigger coupling changes, and occur in clusters that cumulatively cover the entire Mentawai segment at the culmination of each supercycle. It is clear that each Mentawai rupture sequence evolves uniquely in terms of the order and grouping of asperities that rupture, suggesting heterogeneities in fault frictional properties at the ~100 km scale.

1. Introduction and Background

After more than 100 years of earthquake research, anticipation of earthquakes via tectonics-based forecasting has emerged as humanity's best defense against seismic natural disasters. Knowledge of the location, size, and frequency of fault ruptures is required to empower society to plan for and minimize damage from the earthquakes that will inevitably occur. Paleoseismic records are a key part of this body of knowledge, and the longest, most detailed records provide the most accurate understanding of the complete range of fault behavior.

Although paleoseismic records for some faults now stretch for many millennia [e.g., *Clark et al.*, 2013], most do not provide details of fault rupture extent or behavior between ruptures. Study of the Sunda megathrust fault (subduction plate interface) west of Sumatra based on vertical deformation recorded by coral microatolls has produced one of the only paleoseismic records spanning multiple seismic cycles with significant temporal and spatial precision [*Meltzner et al.*, 2010, 2012, 2015; *Sieh et al.*, 2008], and the recent series of megathrust ruptures (Figure 1) has highlighted the extreme earthquake and tsunami hazard in the region. The 700 km long Mentawai segment of the megathrust, between the Batu Islands and Enggano Island, has been characterized by seismic "supercycles," periods of strain accumulation which culminate in a series of ruptures rather than a single end-to-end rupture [*Sieh et al.*, 2008]. In this study, we construct a chronology of interseismic and coseismic deformation on the Mentawai segment, using all available coral microatoll data, in order to examine the variability of fault behavior from one supercycle to the next. The range of behavior we observe informs earthquake forecasts for the region as the current rupture sequence, which began in 2007, unfolds.

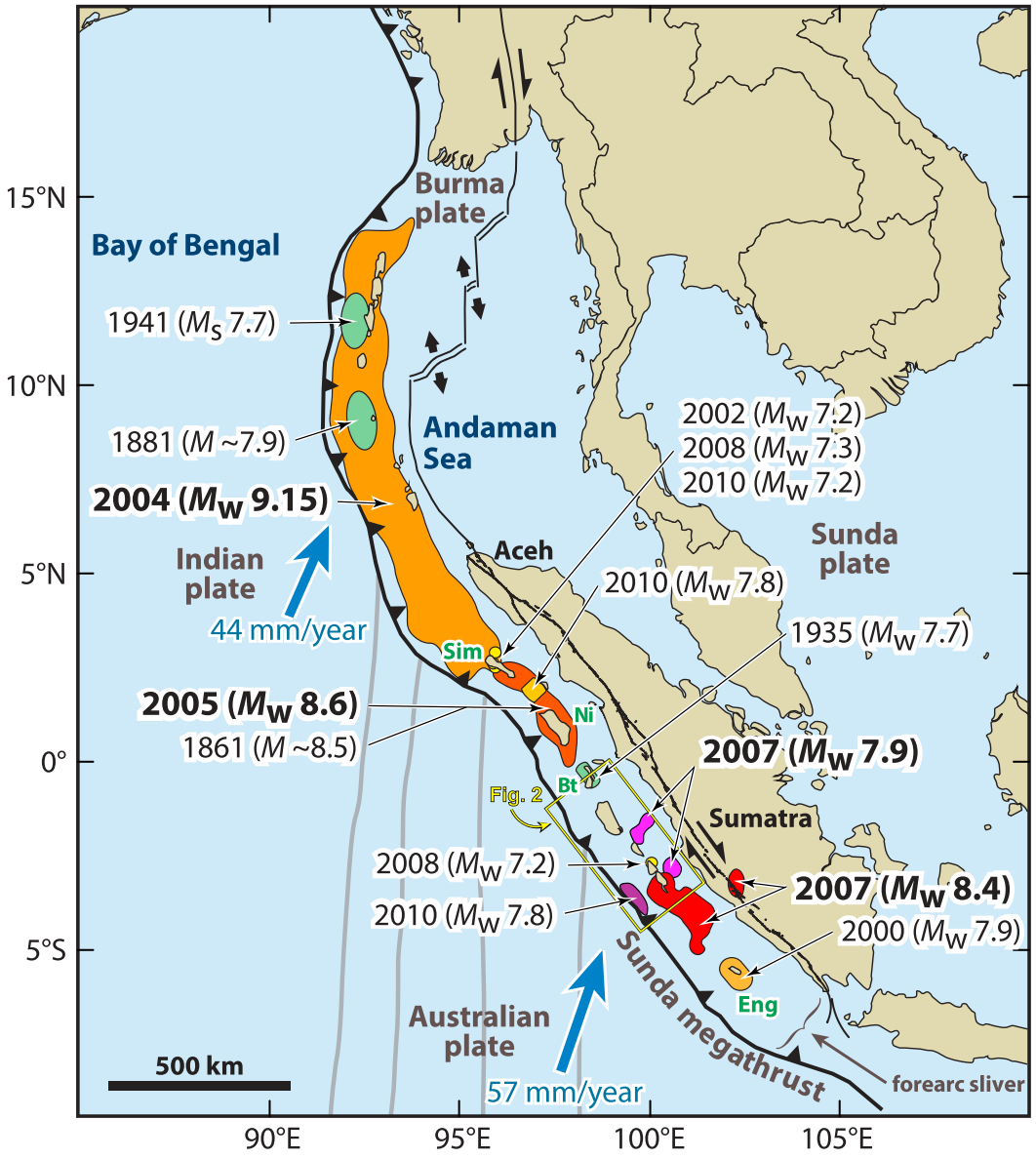

Figure 1. Map of southeast Asia showing recent and selected historical ruptures of the Sunda megathrust. Black lines with sense of motion are major plate-bounding faults, and gray lines are seafloor fracture zones. Motions of Australian and Indian plates relative to Sunda plate are from the MORVEL-1 global model [*DeMets et al*., 2010]. The fore-arc sliver between the Sunda megathrust and the strike-slip Sumatran Fault becomes the Burma microplate farther north, but this long, thin strip of crust does not necessarily all behave as a rigid block. Sim = Simeulue, Ni = Nias, Bt = Batu Islands, and Eng = Enggano. The yellow box (footprint of Figure 2) surrounds the Mentawai Islands. Figure adapted from *Meltzner et al*. [2012] with rupture areas and magnitudes from *Briggs et al*. [2006], *Konca et al*. [2008], *Meltzner et al*. [2010], *Hill et al*. [2012], and references therein.

It is important to note that the term supercycle has now been applied to a wide range of fault behavior, much of which is crucially different from what we observe in the Mentawai case. For instance, *Goldfinger et al*. [2013] includes both rare multisegment ruptures and earthquake clustering under this label, potentially encompassing every type of fault behavior other than the two end-members of quasiperiodic characteristic earthquakes and random rupture extent and timing. We will demonstrate that the Mentawai supercycles culminate with what we might more specifically label "clustered complimentary ruptures": cascading failure of a fault in a series of differing sections. While the Mentawai case does not exhibit characteristic earthquakes per se, its behavior can still be understood under an analogous model.

Sieh et al. [2008] outlined three previous supercycles of the Mentawai segment, culminating in the 1300s, 1600s, and in the historical 1797/1833 doublet. In a previous paper, we examined the historical supercycle (1700s–1800s) and found that while there is no evidence for more than two great earthquakes, the first earthquake in the sequence altered the coupling distribution on the megathrust [*Philibosian et al*., 2014]. We now extend our detailed study to the earlier supercycles, focusing on the sixteenth to seventeenth centuries as far more data are preserved from this period than from earlier times. Throughout this study, we employed the now well-established techniques pioneered by *Taylor et al*. [1987] and further developed by *Zachariasen et al*. [1999, 2000] and *Natawidjaja et al*. [2004] to extract paleoseismic and paleogeodetic data from coral microatolls (hemispheric coral skeletons that grew in the intertidal zone), with updates and improvements following *Meltzner et al*. [2010, 2012], specifically detailed by *Philibosian et al*. [2014]. We determined absolute ages (see Table S1 in the supporting information) using uranium-thorium disequilibrium techniques developed and described by *Edwards et al*. [1988] and *Shen et al*. [2002, 2008, 2012]. As in previous studies, all sampled microatolls are *Porites lutea* or *lobata* unless otherwise specified. *Porites lutea/lobata* microatolls are composed of ~1 mm diameter single-polyp skeletons (corallites). Larger-corallite species, which frequently provide more precise U-Th ages, are tentatively identified as *Goniastrea retiformis* (3–5 mm diameter corallites) or as belonging to the genus *Favia* (~1 cm corallites).

2. Coral Data From the Sixteenth and Seventeenth Centuries

We have doubled the number of sites with coral observations dating to the sixteenth and seventeenth centuries, adding nine new sites to the 10 previously presented by *Sieh et al*. [2008] (Figure 2). We also collected complete coral slices at two of the old sites, Pulau (P.) Pecah Belah B and P. Kumbang, where the record previously consisted only of lone dates obtained from small chiseled samples. (The chiseled samples were originally analyzed by *Zachariasen* [1998] and later mislocated by *Sieh et al*. [2008] on nearby P. Taitanopo and P. Siatanusa.) This greatly expanded data set provides reasonably good coverage of all the Mentawai Islands and reveals a more complex rupture sequence that contrasts with the simpler sequence inferred by *Sieh et al*. from a sparser data set.

Establishing a sixteenth- to seventeenth-century regional coral growth chronology was challenging due to the lack of historical records and the eroded state of many older coral microatolls. Unfortunately the technique of improving age precision by correlating oceanographic die-downs between coral records (employed by *Philibosian et al*. [2014] for the 1797/1833 sequence) was not as useful for the sixteenth- to seventeenth-century records. This is because far fewer specimens are preserved from the sixteenth- to seventeenth-century period, and these older specimens are typically more eroded. While die-down correlation was occasionally useful for aligning multiple coral records from the same site, the limitations led to an inability to clearly identify regional oceanographic events in the sixteenth to seventeenth centuries. We also cannot confidently apply any historical constraints, since reliable records were not kept until the mid-1700s (see section 2.5). Nonetheless, the cluster of closely timed tectonic uplifts provides a set of correlation points between poorly and precisely dated records, resulting in an absolute age uncertainty for the entire chronology of about $\pm$10 years. The assignment of dates to annual bands on coral cross-sectional figures is based on this regional chronology.

As an additional challenge, in this study we encountered an unusually large number of cases (relative to our earlier work) in which U-Th dates gave mutually inconsistent results, either based on counting the number of bands between samples from a given slab, or based on the comparison between microatoll morphologies. While the inconsistent ages generally do not differ wildly from each other, ages that do not match within uncertainty indicate either minor age inaccuracy or underestimated uncertainty. This could be due to thorium isotopic ratios outside our normally assumed range or to interstitial material contaminating the coral skeleton. We prepared our samples for dating by pulverizing, sonicating, and cleaning them in order to eliminate as much interstitial material as possible, but such methods are not perfect. In each case, we present our argument for discarding certain U-Th dates or adopting an interpretation outside the uncertainty bounds of the dates, based on consistency among other dates and similarity of growth histories. The stated age and uncertainty of the youngest preserved annual band on each cross section is based on a weighted average of the U-Th ages, excluding the discarded inconsistent analyses. Note that these youngest-band ages are potentially slightly older than the date of death, as erosion of a few annual bands from a microatoll perimeter is common.

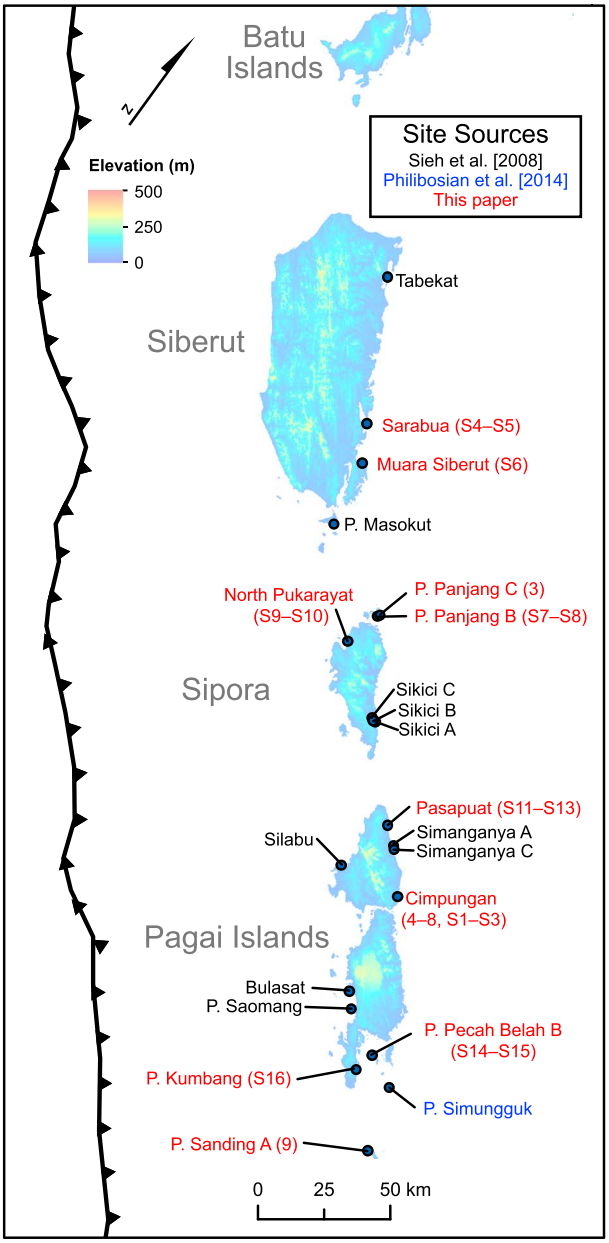

Figure 2. Index map of the Mentawai Islands showing sites with microatolls dating to the sixteenth and/or seventeenth centuries.

We present three representative sites in detail here; data from the other sites appear in the supporting information.

2.1. Pulau Panjang C

Pulau Panjang is the easternmost small island in the archipelago north Sipora Island. We developed three microatoll study sites on P. Panjang, collecting a modern microatoll from site A [*Natawidjaja et al.*, 2007] and a sixteenth-century fossil microatoll from site B (see Figures S7 and S8 in the supporting information), but coral records from site C present the clearest and most complete history of vertical deformation in the area. Site C lies in a small cove on the northeast coast of P. Panjang (Figure 3a). The cove contains dozens of microatolls. We identified four distinct generations of microatolls based on elevation, species, and morphology: low-lying cup-shaped *Porites* microatolls, cup-shaped Favids at slightly higher elevations, a much higher-elevation group of Favids which grew on top of the older *Porites* microatolls, and modern, living microatolls displaying clear evidence of uplift during the 2007 M_w 7.9 earthquake.

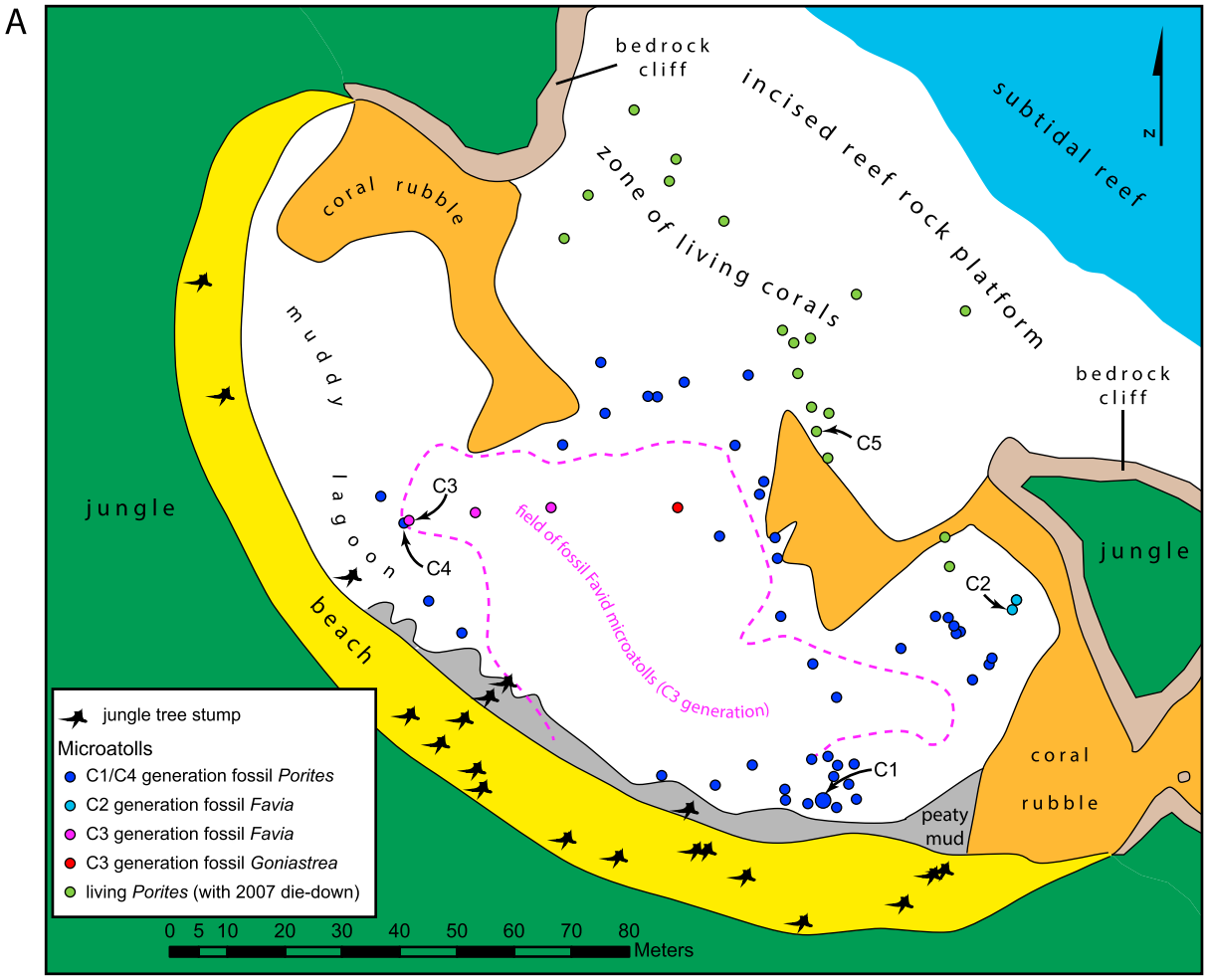

Figure 3. Data from Pulau Panjang site C. (a) Map of the site, a bay on a small island north of Sipora. Four generations of microatolls record several uplifts and intervening subsidence of the site. The C1/C4 and C2 microatolls died during the late sixteenth and mid-seventeenth centuries, respectively. The C3 group grew on top of the older groups (C3 grew on the rim of C4) and then died due to uplift in the historical 1797 earthquake. Modern microatolls display clear evidence of uplift during the 2007 M_w 7.9 earthquake. A peat layer and many tree stumps sandwiched between an ancient coral platform and the modern beach are further evidence of cycles of uplift and subsidence. (b) Cross section of microatoll PJG12-C1 showing steady interseismic subsidence until the coral was uplifted and killed in about 1597. (c) Cross section of Favid microatoll PJG12-C2. This head was hemispherical prior to an uplift in ~1597, which was followed by 60 years of interseismic subsidence. Finally, a second uplift killed the colony. (d) Growth history of C1, C2, and C4 illustrating the two uplift events separated by ~60 years. The interseismic deformation rates before and after the 1597 uplift were similar, although the subsidence rate may have increased slightly following that event.

Dates and cross sections from one or two specimens from each population allow us to reconstruct the chronology of coral growth at the site. The highest fossil population (represented by sample PJG12-C3) was killed by uplift during the historical 1797 earthquake (see *Philibosian et al.* [2014], who also include analysis of the sampled modern microatoll C5). The two lower populations died in the 1600s during the preceding rupture sequence. The *Porites* C1 experienced gradual submergence before dying around the year 1600 (Figure 3b). The Favid C2 was a hemisphere (having never hit its highest level of survival, or HLS) before it was partially uplifted around the year 1600 (Figure 3c). Sixty years of steady submergence followed until the coral died around the year 1660, presumably due to a second sudden uplift. The partial uplift of C2 was very likely contemporaneous with the death of C1. The much more precise age of C2 (common for large-corallite species) constrains the complete history within a narrow interval; we assign the exact years of 1597 and 1658 to the two uplifts based on our synthesis of all the coral records throughout the Mentawai region.

Figure 3d plots the growth histories of these corals at their relative elevations as measured in the field, including PJG12-C4, a second sampled head in the same generation as C1 (the cross section of C4 was included by *Philibosian et al.* [2014]). C1 apparently settled 5–10 cm into the substrate relative to C4, and C4 may have

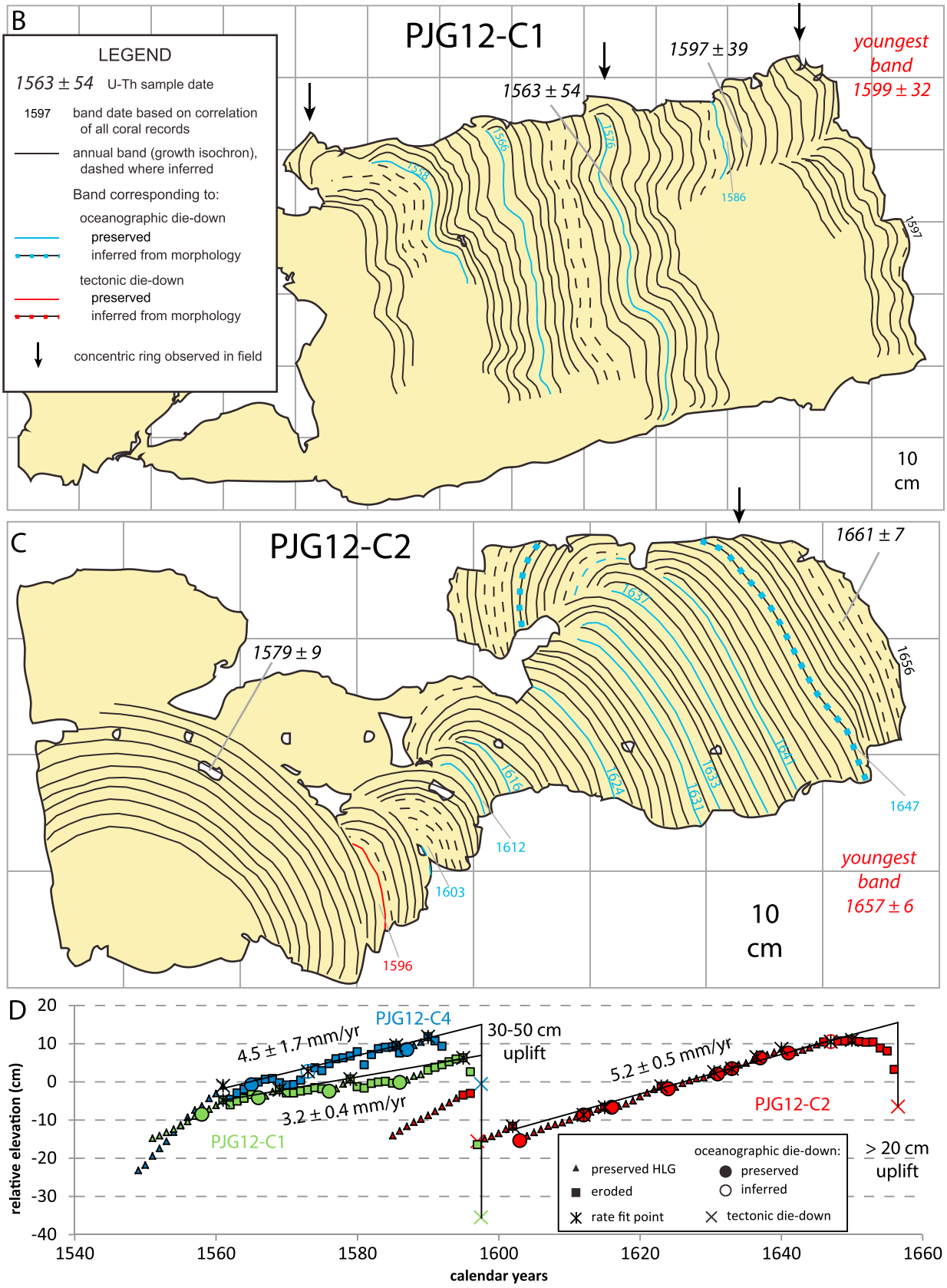

Figure 3. (continued)

settled as well, leaving the total uplift in 1597 somewhat uncertain. Based on the current relative elevations of the microatolls the uplift was 30 cm, but the vertical thickness of C1 suggests >50 cm uplift. The HLS for Favid corals is sometimes 10–15 cm higher than *Porites lutea/lobata*, so it is possible that C1 died while the perimeter of C2 remained alive at a slightly higher elevation. Considering all these factors, we estimate the 1597 uplift at 40 ± 10 cm at this site. The 1658 uplift must have been at least 20 cm, but the full amount cannot be measured directly.

2.2. Cimpungan

We developed three closely spaced sites near the village of Cimpungan on the southeast coast of North Pagai. At sites B and C, hundreds of fossil microatolls cover a muddy lagoon and rubbly coral platform (Figure 4). Tilting and disparate elevations show that many microatolls have settled into the muddy substrate, making it difficult to distinguish populations based on elevation. Therefore, we instead classify them based solely on differences in morphology. Numerous microatolls at this site exhibit a conical hat shape, indicating a period of gradual uplift or several small uplifts closely spaced in time, while others have the more typical cup shape indicative of gradual interseismic subsidence.

We collected slices of five microatolls at site B and two more at site C, all of which lived roughly contemporaneously and died in the seventeenth century. Figure 5 shows cross sections of two representative specimens. CMP08-B1 has a highly eroded top, but its concentric rings nevertheless define a period of submergence followed by a period of emergence. Due to erosion it is unclear exactly when the first ~10 cm of emergence occurred, but an additional ~20 cm emergence clearly occurred suddenly around the year 1613. Following the second emergence, gradual uplift continued for 6 years (totaling about 5 cm) until submergence resumed. Finally, a third uplift of at least 25 cm killed the colony completely in ~1631. (As above, the exact years of these events are assigned based on our complete analysis of all Mentawai corals from this supercycle. Also, at the Cimpungan site there were enough well-preserved microatolls to allow correlation between specimens based on major oceanographic die-downs.)

The less-eroded microatoll CMP08-B4 (Figure 5b) preserves a clearer history of the period corresponding to the eroded inner portion of B1, with several oceanographic die-downs defining the period of interseismic subsidence prior to a likely sudden uplift in ~1597. Minor amounts of subsidence and uplift followed until the coral was killed by a second sudden uplift, likely corresponding to the second (20 cm) die-down of B1. The B4 head was too thin to survive this uplift and the living perimeter died completely. Based on the B4 record, we infer that the first 10 cm uplift on B1 also occurred in 1597.

The five other microatolls sampled here record various parts of the same history, with the cup-shaped microatolls dying due to the 1597 uplift and the hat-shaped ones due to the 1613 uplift (see Figures S1–S3 and Text S1 in the supporting information). Although B1 is our only sampled microatoll that survived 1613 and died in 1631, others at the site had a similar morphology. At site A, a few hundred meters north of site C, we found another large field of mixed hat- and cup-shaped microatolls (Figure 6). While the hat-shaped group (represented by samples CMP08-A1 and A3; see Figure S3) corresponds to the same period as the B/C populations, the cup-shaped group represented by CMP08-A2 is significantly younger. A2 records 50 years of rapid interseismic submergence leading up to its emergence and death sometime in the eighteenth century (Figure 7). While the radiometric dating of this sample is quite imprecise, we infer that it likely died in ~1703 based on more precise ages of microatolls at other sites.

The 10 coral growth records derived from Cimpungan microatolls can be correlated with each other based on the timing of both tectonic and oceanographic die-downs (Figure 8). The period of emergence (which appears to have included at least three sudden uplifts in 1597, 1613, and 1631) must have been contemporaneous across all the records, and the large die-down in 1569 also provides a robust tie-point. The 1569 die-down has oceanographic characteristics in that the coral had uninterrupted recovery growth for the next decade until it reached its prior HLS; however, its large magnitude (15 cm) and the tilting of head B2 at that time (Figure S1) leads us to at least consider the possibility that it was tectonic.

In Figure 8b, we overlay all the coral records at their inferred original relative elevations (corrected for settling into the mud) to illuminate the complete history of tectonic vertical deformation. After at least 50 years of rapid interseismic subsidence, the uplift sequence may have begun with a small uplift in 1569 (which was recovered in no more than a decade). Emergence dominated between 1590 and 1631, punctuated by at

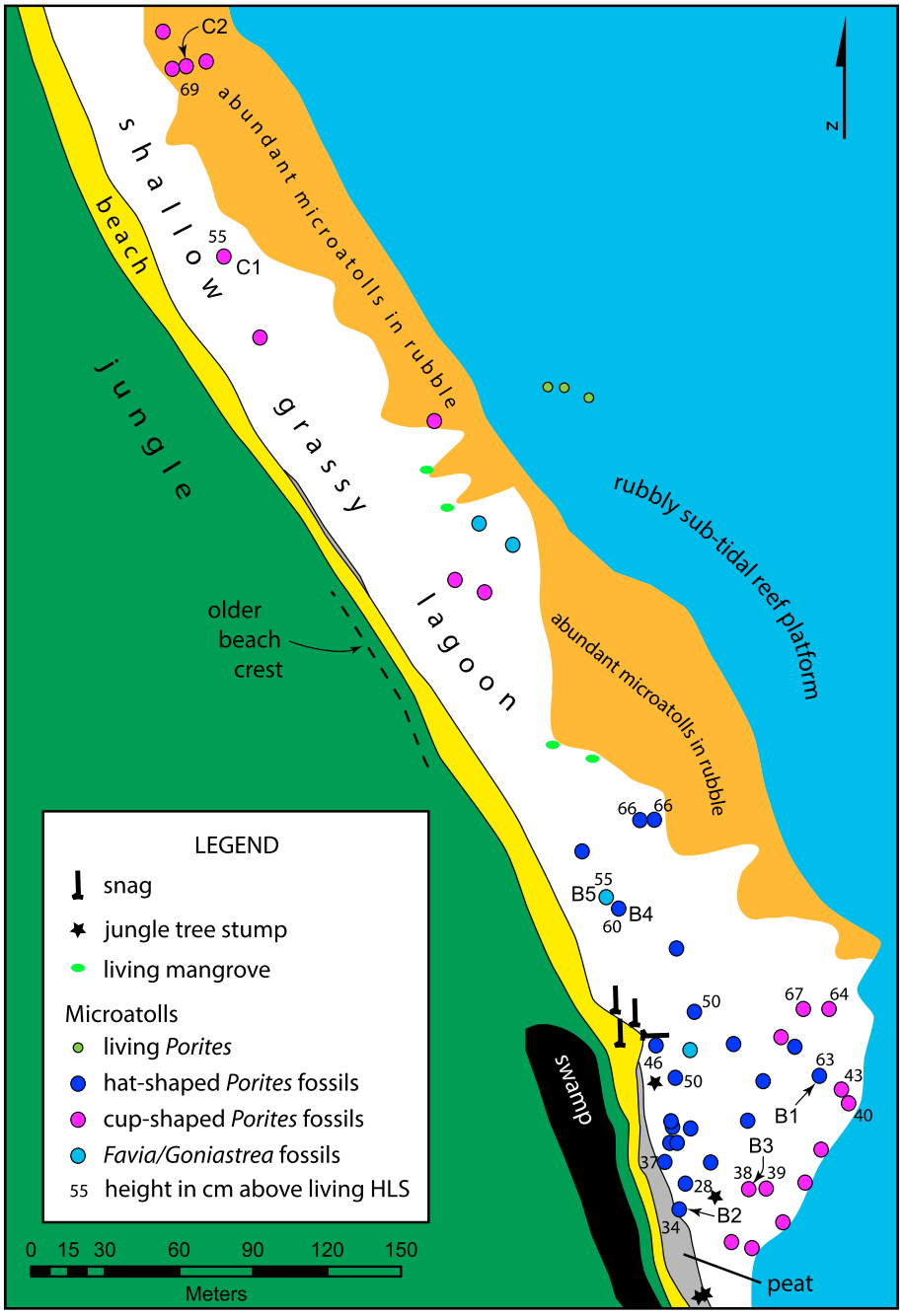

Figure 4. Map of Cimpungan sites B and C on the east coast of North Pagai. The peat eroding from beneath the beach likely accumulated after a major coseismic uplift, covering and preserving many microatolls. Jungle trees grew on the coral platform at that time, but have since drowned due to interseismic subsidence. Surveyed elevations of microatolls illustrate that many have settled into the muddy substrate, particularly toward the southern end of the microatoll field. An old beach crest may correspond to the population of fossil microatolls. All the microatolls collected here died during the seventeenth century.

least three relatively large sudden uplifts in 1597, 1613, and 1631, with a total uplift of ~70 cm. Rapid interseismic subsidence then resumed until a final uplift of at least 22 cm occurred in 1703. While the 1597 uplift may correlate with the first event at P. Panjang, the prolonged period of multiple uplifts clearly did not occur at P. Panjang. Conversely, there is no evidence of uplift at Cimpungan in 1658. We will see that these noncorrelations between two sites ~100 km apart have important implications for the geographical extent of individual megathrust ruptures during this period.

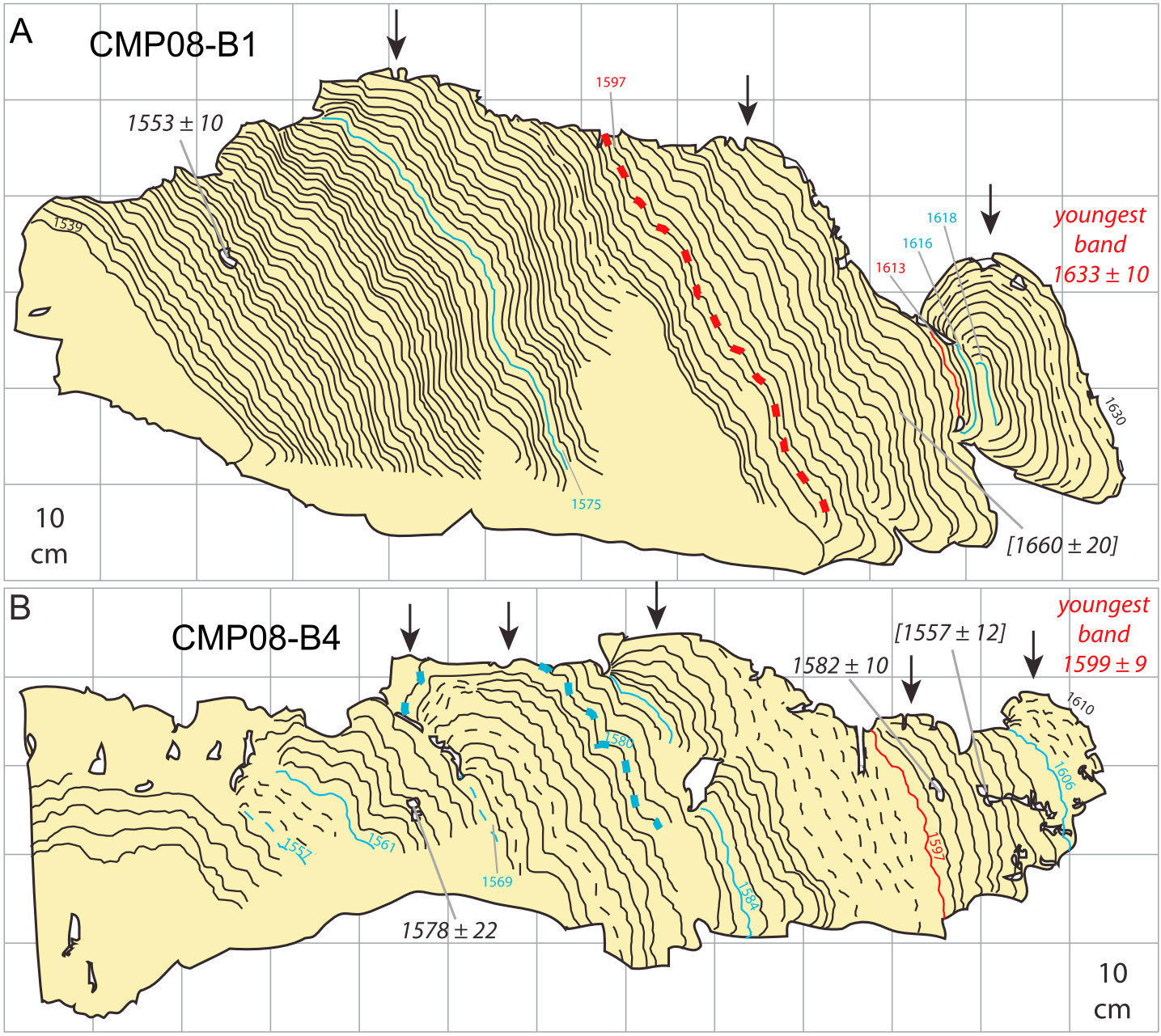

Figure 5. Two representative slab cross sections out of 10 collected at Cimpungan (symbols as in Figures 3b–3d). (a) The eroded top of CMP08-B1 defines a period of submergence followed by two emergence events, the first about 10 cm and the second about 20 cm. Following the second emergence, gradual uplift continued for 6 years until submergence resumed. A third uplift of at least 25 cm killed the colony completely. The two U-Th dates obtained for this coral are incompatible given the very clear band counting; we use the 1553 ± 10 date as it is more consistent with the dates of other similar corals. (b) The less eroded CMP08-B4 preserves a clearer history of the period corresponding to the eroded inner portion of B1, but this thinner coral was killed completely by the second of the three emergence events. We exclude the 1557 ± 12 date from our analysis as it is inconsistent with the other two dates from this specimen as well as with dates from similar nearby corals.

2.3. Pulau Sanding

Our southernmost site is on the southwest side of the small island of Sanding, 30 km southeast of South Pagai (Figure 9a). More than a meter of uplift during the 2007 M_w 8.4 earthquake killed all the modern corals growing on the broad reef platform. The site also features two populations of fossil microatolls, one group scattered over the reef platform and the second close to the beach. Based on analysis of SDG10-A3, the scattered population died due to uplift in the historical 1833 earthquake [*Philibosian et al.*, 2014].

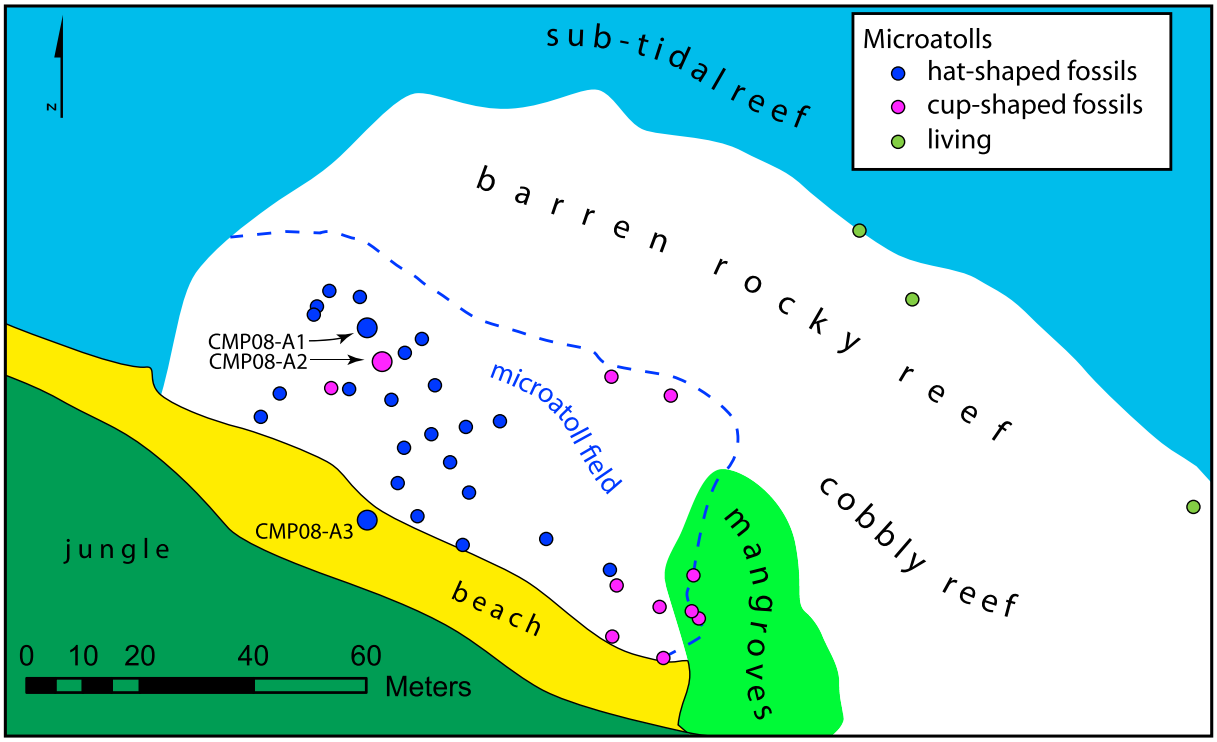

Figure 6. Map of Cimpungan site A on the east coast of North Pagai. The hat-shaped generation died during the early seventeenth century and the cup-shaped generation died in the early eighteenth century.

We sampled two of the microatolls close to the beach, SDG10-A1 and A2. A2 (Figure 9c), which was partially uplifted at least twice (in about 1597 and 1613) and experienced additional uplift for several years after 1613, until subsidence resumed. Finally, the colony was killed in about 1631. A1 (Figure 9b) and has an eroded central dome which was exposed by a tectonic uplift, followed by at least 20 years of subsidence. The outer rim was detached from the central part of the microatoll, so its original elevation is uncertain. However, the rim records continuing subsidence until the colony was killed at the beginning of the eighteenth century, presumably by a large uplift. Based on the band counting, the two U-Th ages obtained from A1 are mutually inconsistent. Given the lack of definite uplift events between the inner dome and outer perimeter of A1, it seems most likely that the preserved first uplift of A1 is the last of the three recorded by A2, and thus occurred in 1631. This interpretation is most consistent with the relative elevations of the microatolls and with three of the four U-Th dates, which are remarkably precise for *Porites lutea* or *lobata* specimens.

The complete history (Figure 9d) includes three small uplifts totaling at least 45 cm during the early 1600s, followed by 70 years of slow interseismic subsidence culminating in a larger uplift at the beginning of the eighteenth century. As the spacing between the uplift events is very similar to that observed at Cimpungan, and such an interpretation is consistent with the U-Th dates, we conclude that the four uplift events recorded at P. Sanding are the same four events recorded at Cimpungan. The detached rim of SDG10-A1 makes it unclear whether there was any uplift at P. Sanding coinciding with the 1658 uplift at Pulau Panjang; the maximum amount that could have occurred is 20 cm.

2.4. Other Sites

Coral growth histories and dates of death from the other 18 sites all fit into the chronology framed by the data from P. Panjang C, Cimpungan, and P. Sanding. All of the coral data are compiled in Figure 10, which is supported by details of the new sites and coral cross sections in supplementary Figures S4–S19. We briefly summarize each site below, from northwest to southeast.

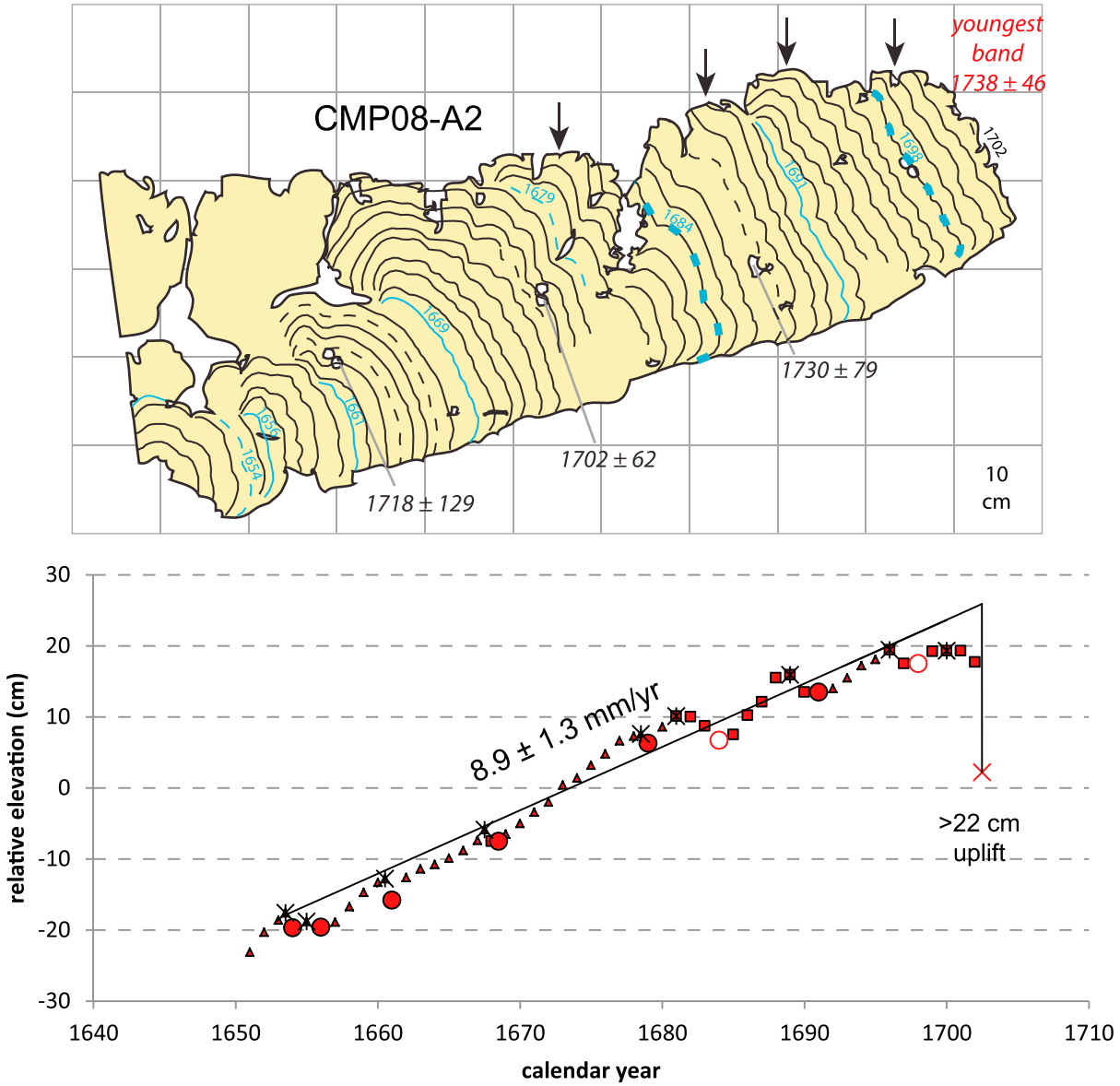

Figure 7. Cross section and growth history plot of CMP08-A2, a representative of the younger cup-shaped population at Cimpungan site A. Symbols as in Figures 3b–3d. The period of growth does not overlap with the older populations. This coral records fairly rapid submergence until an uplift killed the colony in the early 1700s.

2.4.1. Tabekat

A chiseled sample from a small microatoll yields a youngest-band date of 1648 ± 26, consistent with uplift and death in 1658 [*Sieh et al.*, 2008].

2.4.2. Sarabua

A precisely dated microatoll represents a population that died within a few years of 1658. No significant uplift occurred between 1597 and 1658 (Figures S4 and S5).

2.4.3. Muara Siberut

The population of corals represented by MSB10-A3 died in about 1658; two other more isolated microatolls died in the 1630s for unknown reasons. No significant uplift occurred between 1597 and 1658 (Figure S6).

2.4.4. P. Masokut

A small microatoll has a youngest-band date of 1668 ± 29, consistent with uplift and death in 1658 [*Sieh et al.*, 2008].

2.4.5. P. Panjang B

A microatoll recording a long history of subsidence has a youngest-band date consistent with uplift and death in 1597. There is no evidence of uplift in 1569 (Figures S7 and S8).

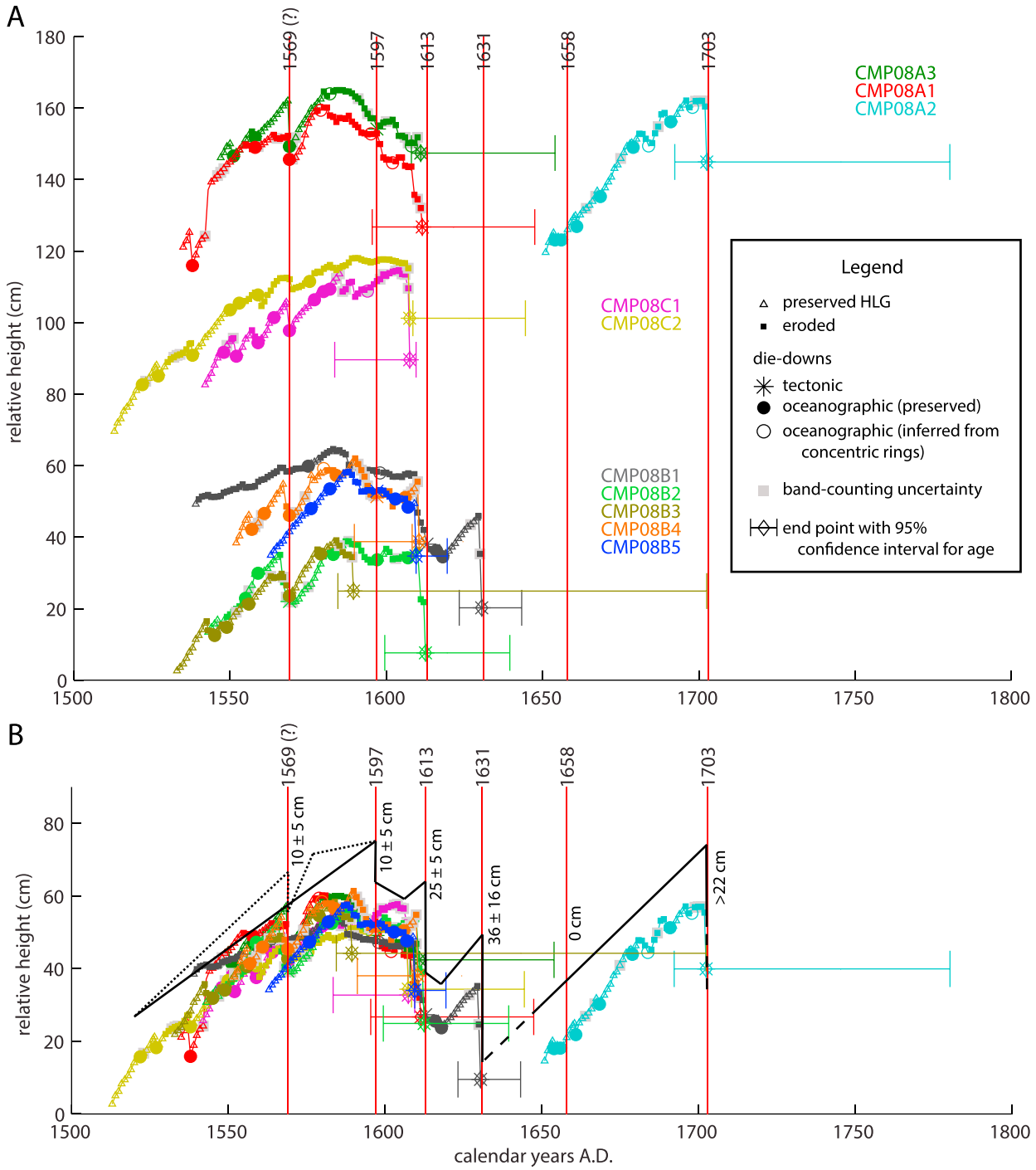

Figure 8. Synthesis of 10 coral records from Cimpungan, shifted within their age uncertainties to form a self-consistent history. (a) Records split into the three subsites with those from each subsite plotted at their observed relative elevations in the field. All of the sampled coral heads at site B have clearly settled into the substrate relative to B1, particularly B2 and B3 which have sunk ~30 cm. (b) When all records are restored to their likely original heights, the complete history of tectonic vertical deformation becomes clear (heavy black line, offset above coral records for visual clarity). The dotted black line shows an alternate scenario in which the large 1569 die-down is interpreted as a tectonic rather than oceanographic event.

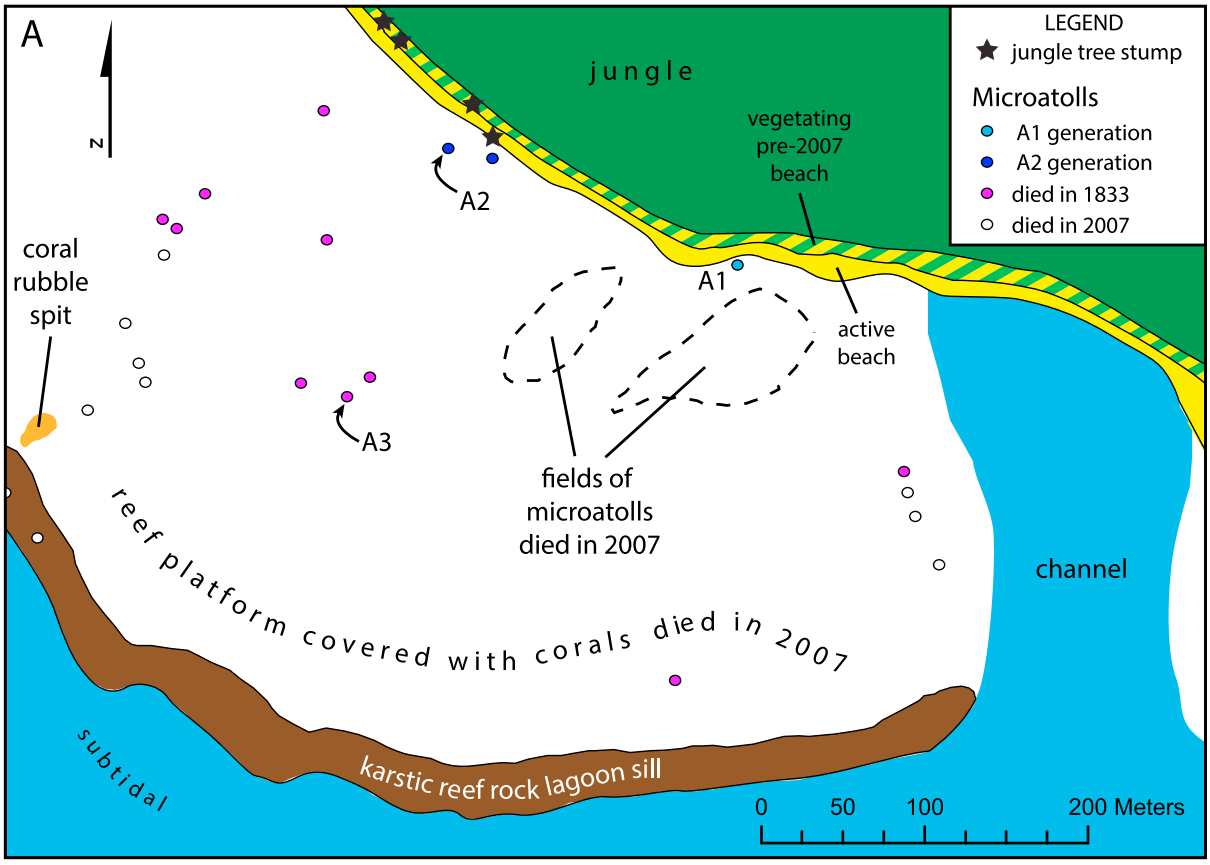

Figure 9. Data from Sanding Island. (a) Map of the site on the south coast of the island. Here the entire reef platform was killed due to ~1 m of coseismic uplift in 2007. Stumps of jungle trees protruding through the beach are evidence of interseismic subsidence prior to 2007; since the earthquake, that area has been re-vegetating. A population of fossil microatolls scattered over the middle of the reef platform died due to uplift in the 1833 earthquake [see *Philibosian et al.*, 2014]. Other fossil microatolls close to the beach died in the seventeenth century. (b) Cross section of SDG10-A1, which experienced a tectonic uplift early in its life, followed by slow subsidence until it was killed by a second uplift. The outer rim is detached so its original elevation is unclear. The two U-Th ages are mutually inconsistent given the band counting; we use the 1679 ± 5 date as this is more consistent with the A2 record and with records at other sites. Symbols as in Figure 3b. (c) Cross section of SDG10-A2, which experienced three closely spaced, small tectonic uplifts, the last of which likely coincided with the first event recorded by A1. Symbols as in Figure 3b. (d) Growth histories of the two microatolls, with the outer rim of A1 restored 10 cm upward to its likely original elevation. The same four uplift events recorded at Cimpungan are present in these records. Symbols as in Figure 3d.

2.4.6. North Pukarayat

A large hat-shaped microatoll records two large uplifts separated by ~40 years. We infer that these occurred in 1658 and 1703, although this interpretation is at odds with one of the U-Th dates. If our interpretation is correct, this is the northernmost record of the 1703 uplift. An alternative interpretation (consistent with all the dates) is that the microatoll was transported by a tsunami in 1613 (resulting in the appearance of a large uplift) and the second, true uplift occurred in 1658. This alternative interpretation would not significantly change the overall uplift distribution in either 1658 or 1703, as the amount of uplift on northern Sipora appears to have been similar in the two events, based on records from other sites. (Figures S9 and S10).

2.4.7. Sikici C

Four poorly dated microatolls were presented by *Sieh et al.* [2008], who inferred that the population died in the latest 1500s (at the same time as a large uplift recorded by more precisely dated corals at Sikici B). We collected two chiseled samples (SKC08-C2 and C5) from large-corallite species microatolls in the same population as the earlier SKC03-C samples. Our more precise dates (see Table S1) confirmed that the population died in the latest 1500s, consistent with the 1597 event. Based on the previously published data, there is no evidence of uplift in 1569.

2.4.8. Sikici B

Sieh et al. [2008] presented three cross sections from two microatolls which collectively record a nearly a century of subsidence ended by an uplift around 1597, followed by ~60 years of stability. Erosion obscures the

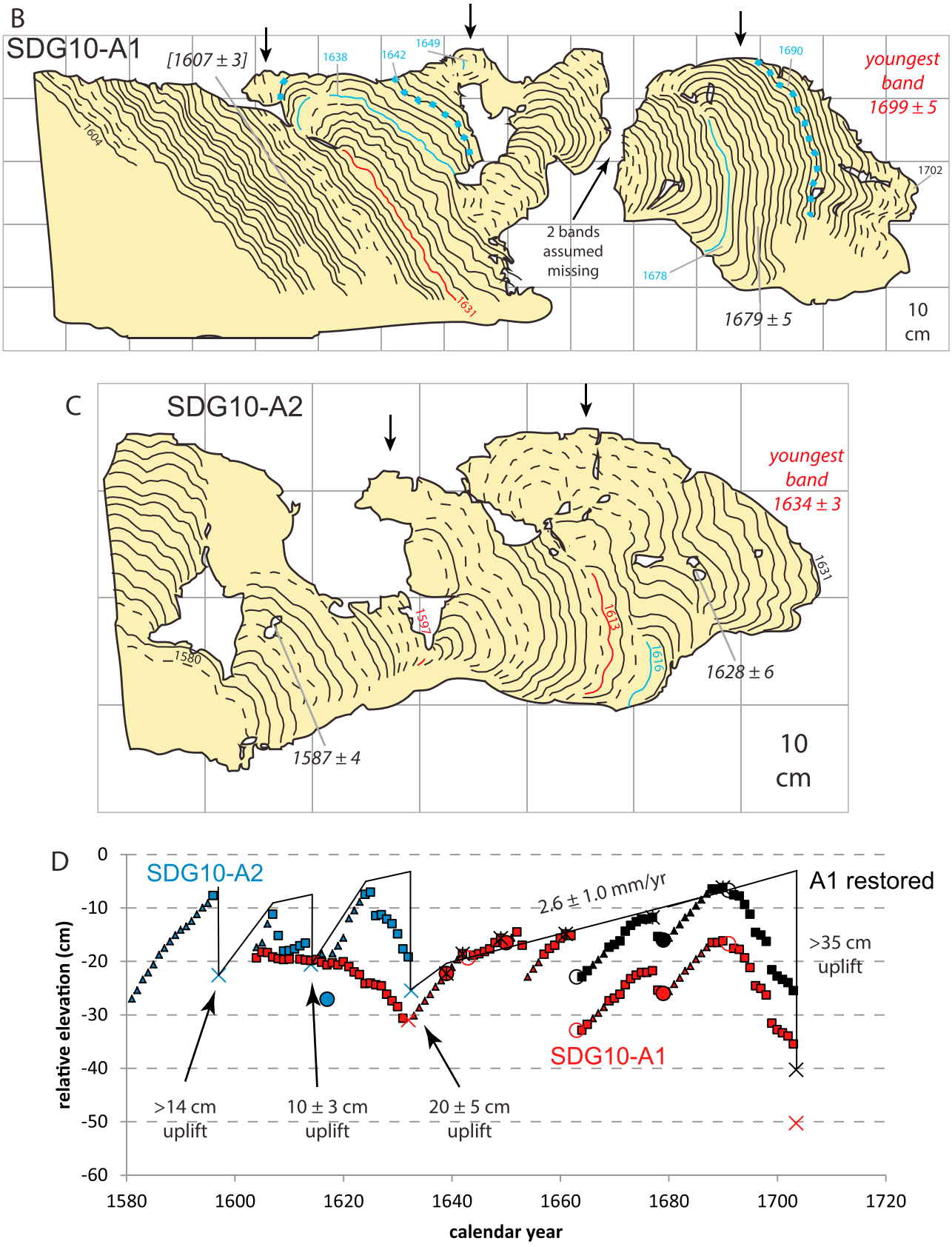

Figure 9. (continued)

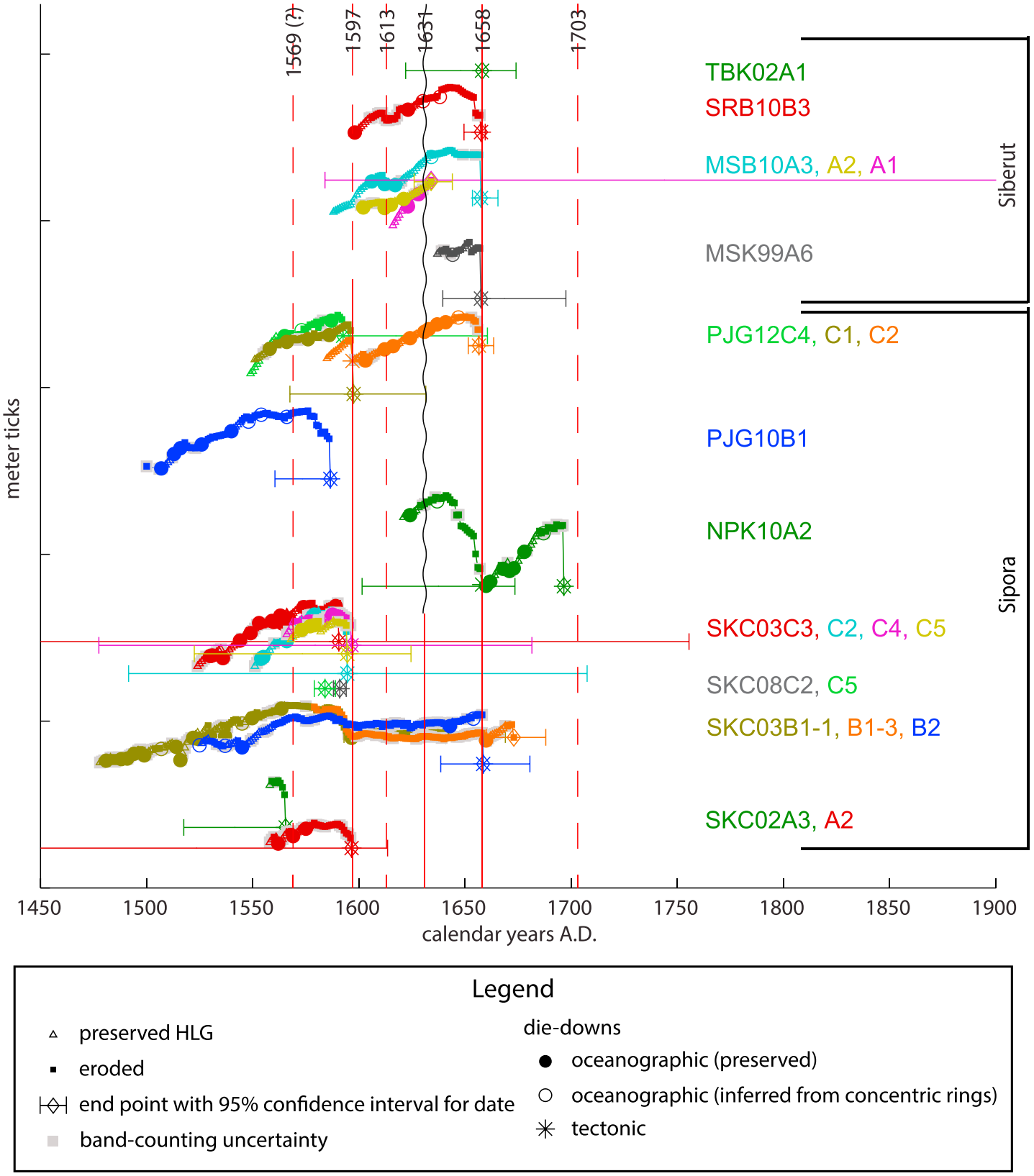

Figure 10. All coral records from the sixteenth and seventeenth centuries, with sites ordered from NW to SE and each site vertically offset from the next. Each coral record is shifted within its age uncertainty bounds to achieve the best overall correlation between records at all sites. The vertical lines indicate inferred tectonic uplifts, solid red where clear, dashed red where small or unconstrained, and wavy black where precluded.

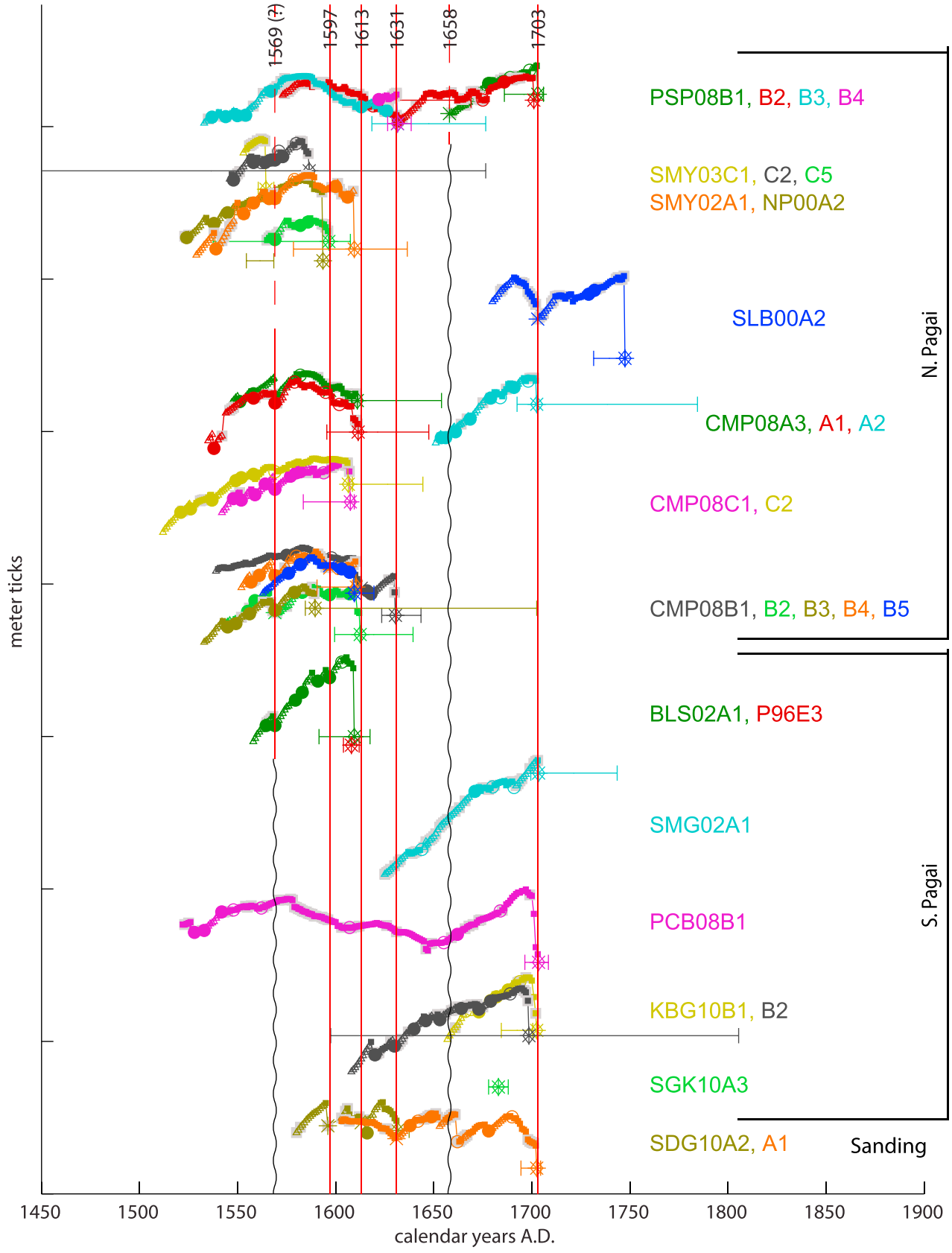

Figure 10. (continued)

detailed history, but any uplifts between 1597 and 1658 must have been small (<10 cm). The death of SKC03-B2 is consistent with uplift in 1658 and would thus be the southernmost record of that event. SKC03-B1 apparently survived this uplift, dying about 15 years later than B2. The final death of the thin living rim of B1 may have been purely due to oceanographic fluctuations or environmental stress; it was only ~10 cm high. There are no other records that suggest an uplift event in the 1670s.

2.4.9. Sikici A

One of the two microatolls presented by *Sieh et al*. [2008], SKC02-A2, has a very large age uncertainty but its morphology is similar to the other Sikici samples that died in 1597. The second microatoll, SKC02-A3, was 50 cm higher in elevation than A2 and has a date of death consistent with the postulated 1569 event at Cimpungan (see Figure 8). However, the continuous records from site B preclude any large uplift within the age range of the death of A3. There are two possible interpretations: the age of A3 is incorrect, or A3 died due to nontectonic causes and A2 settled relative to A3.

2.4.10. Pasapuat

The combination of four microatoll records reveals a period of subsidence in the mid-1500s, a period of uplift corresponding to the 1597, 1613, and 1631 uplift events, and a resumption of subsidence until the final uplift in 1703. Although any uplift in 1658 must have been small, one of the microatolls was overturned in 1658, perhaps due to a tsunami generated farther north. A small uplift may have occurred in 1569 (Figures S11–S13 and Text S1).

2.4.11. Simanganya A/C

Due to widespread settling, the original relative elevations of the five microatolls presented by *Sieh et al*. [2008] are unclear. Similar morphologies suggest that SMY03-C2, SMY03-C5, and NP00-A2 originally grew at the same elevation and died in 1597 (although this is at odds with the age of NP00-A2). SMY02-A1 records a small uplift followed by a larger uplift that killed the colony, consistent with the 1597 and 1613 events. This was the only specimen presented by *Sieh et al*. [2008] that hinted at the period of multiple uplift events during the early 1600s. Similar to SKC02-A3, SMY03-C1 has a date of death consistent with 1569 but large uplift at that time is precluded by other Simanganya records.

2.4.12. Silabu

A midlife uplift of a formerly hemispherical microatoll, SLB00-A2, occurred in 1693 ± 8 according to *Sieh et al*. [2008]. We assign a slightly larger uncertainty based on the unclear annual banding in this specimen [see *Natawidjaja et al*., 2006], making the uplift date (barely) consistent with the 1703 event. This microatoll survived the uplift and died for unknown reasons in the mid-1700s.

2.4.13. Bulasat

A microatoll (BLS02-A1) recorded 50 years of subsidence before being killed by an uplift of at least 50 cm [*Sieh et al*., 2008]. The youngest-band age of 1600 ± 13 is consistent with death in either 1597 or 1613. We favor the interpretation that it died in 1613, since 1613 is clearly the larger of the two uplifts at the nearest neighboring site of Cimpungan. An even more precise date of 1608 ± 4 from a chiseled sample (P96E3) in the same population further supports the 1613 date assignment. A few centimeters of uplift may have occurred in 1597 as well as in 1569.

2.4.14. P. Saomang

A microatoll (SMG02-A1) recorded subsidence throughout the late 1600s until its death [*Sieh et al*., 2008], which is consistent with uplift in 1703. Presuming this interpretation is correct, there was clearly no uplift in 1658 at this site.

2.4.15. P. Pecah Belah B

A slab collected from a population of huge hat-shaped microatolls provides the longest continuous history of the 1500s and 1600s. Subsidence persisted during the mid-1500s (with little or no uplift in 1569), followed by a period of emergence in the early 1600s. Although the details are obscured by erosion, at least two and possibly all three of the 1597, 1613, and 1631 events caused uplift at this site. Although emergence continued until ~1650, there is no indication of uplift in 1658. The precise age of the microatoll is consistent with death in 1703 (Figures S14 and S15).

2.4.16. P. Kumbang

Two microatolls represent a population with ages consistent with death in 1703. Subsidence persisted throughout the 1600s with a potential small uplift in 1631 and none in 1658 (Figure S16).

2.4.17. P. Simungguk

A chiseled sample from a highly eroded microatoll is consistent with death in 1703 [*Philibosian et al*., 2014].

Given the dating uncertainties and our various assumptions, alternate scenarios for the chronology of tectonic events during the sixteenth and seventeenth centuries are possible, though perhaps not as plausible. In particular, it is always possible to explain the data with a larger number of events that each affected a smaller area, up to the extreme case where each site is affected by its own series of events independent from the others. In an application of Occam's razor, we choose the scenario involving the smallest number of events that can plausibly explain all the data.

2.5. Historical Constraints

Unfortunately, historical records that would help to more precisely constrain the dates of these events are scanty. Local Indonesian or Malay records from the colonial period rarely mention earthquakes, perhaps because seismic shaking typically did not damage their flexible wooden or thatched buildings [*Reid*, 2015]. Therefore, historical evidence of earthquakes in this period comes mainly from reports of damage to European trading posts, which were typically masonry buildings. Although the Dutch established a trading post at Padang in 1657 and the British at Bengkulu in 1688, reports at both locations were sporadic until the mid-1700s and typically only mention earthquakes if they damaged company property.

Based on a compendium in Dutch scientific literature, *Newcomb and McCann* [1987] mention an earthquake report from Padang in 1681, the earliest in their list, but no others until 1756. *Harris and Major* [2016] also list this earthquake (based on the same source material). Based on the primary sources of Dutch East India Company (Vereenigde Oost-Indische Compagnie) mission reports, *Reid* [2016] does not list 1681 but lists two other earthquake reports from Padang in 1691 and 1697. Given the U-Th age uncertainties, the latest event in our sequence (to which we assign the year 1703) could actually have occurred in 1697, or in a stretch 1691, but it is unlikely that any of our events correspond to the 1681 report. Regardless, it is unclear from these early, brief descriptions whether the historical earthquakes in question were megathrust events or were perhaps more similar to the 2009 Padang earthquake. Therefore, we cannot confidently apply any historical constraints to our dates. However, the lack of tsunami reports in these records does suggest that the ~1658 and ~1703 megathrust events did not produce large tsunamis on the coast of Sumatra; they were likely similar in that respect to the 2007 Bengkulu earthquake.

Interestingly, one historical record that does potentially coincide with the ~1658 event is a report of a potential tsunami in Banda Aceh in 1660 [*Reid*, 2016]. While it is very unlikely that a Mentawai event would have caused a large tsunami in Banda Aceh, especially given the lack of tsunami reports at more proximal trading outposts, the Banda Aceh event could be related. As evidenced by the close succession of Sunda megathrust ruptures since 2004, ruptures on one segment may trigger ruptures on other segments. If the 1660 Banda Aceh report does truly describe a tsunami, the instigating earthquake could have been part of a multisegment rupture cascade, either triggering or triggered by the ~1658 Mentawai event.

3. Discussion and Modeling of Coseismic and Interseismic Behavior in the Sixteenth and Seventeenth Centuries

3.1. Distribution of Coseismic and Interseismic Deformation

Having synthesized all the coral records from the sixteenth and seventeenth centuries into a self-consistent, most-plausible chronology, we can now analyze the uplift pattern for each individual event as well as the interseismic subsidence patterns. The relevant vertical deformation data is compiled in Table 1.

3.1.1. Coseismic Deformation

Figure 11 illustrates the spatiotemporal progression of the five (possibly six) uplift events. One important caveat is that without historical records and with ~1 yr temporal precision, we cannot prove that these uplifts were necessarily associated with earthquakes. Uplift during aseismic "slow earthquakes" or combinations of coseismic and postseismic uplift (over a period of months) are also possible interpretations. However, given the numerous recent and historical megathrust earthquakes in this area, the uplift events we document most likely happened during earthquakes and we interpret them as such.

3.1.1.1. 1569

Several corals in the central Mentawai Islands exhibit large die-downs of 10–30 cm at this time. Given that most corals apparently recovered rapidly from this event and that it seems to have had different effects on different corals at the same site, it is likely a strong Indian Ocean Dipole (IOD) oceanographic event. Strong positive IOD events can lower sea surface height in the Mentawai Islands by several tens of centimeters for

Journal of Geophysical Research: Solid Earth

10.1002/2016JB013560

Table 1. Coseismic Uplifts and Interseismic Vertical Deformation Rates in the Sixteenth to Seventeenth Centuries[a]

Latitude	Longitude	Full Name	Site Code	1500s Rate	1600s Rate	1569	1597	1613	1631	1658	1703	Projected	Projection Source Site
−1.040	98.947	Tabekat	TBK							>30			
−1.498	99.187	Sarabua	SRB		−4.7 ± 1.6			0 ± 5	0 ± 3	>30			
−1.606	99.234	Muara Siberut	MSB		−5.6 ± 3.0			0 ± 5	0 ± 3	>30			
−1.827	99.294	Masokut	MSK		−3.8					>35			
−1.982	99.600	P. Panjang C	PJG-C	−3.3 ± 0.4	−5.2 ± 0.5	0 ± 3	40 ± 10	0 ± 3	0 ± 3	>20 (40)	(25)	63 ± 22	same
−1.987	99.602	P. Panjang B	PJG-B	−4.7 ± 1.1		0 ± 5	>40 (?)						
−2.123	99.565	North Pukarayat	NPK		−10.9 ± 2.3					55 ± 10	>40 (?)	40 ± 6	same
−2.274	99.784	Sikici C	SKC-C	−5.7 ± 1.0		0 ± 3	>50						
−2.286	99.785	Sikici B	SKC-B	−4.0 ± 0.3	−1.6	0 ± 5	25 ± 10	5 ± 5	0 ± 5	15 ± 5		42 ± 5	same
−2.289	99.802	Sikici A	SKC-A			25 (?)	>15						
−2.550	100.044	Pasapuat	PSP	−5.9 ± 2.5	−2.3 ± 2.6	0 ± 3	10 ± 5	15 ± 5	20 ± 5	0 ± 5	>20	43 ± 11[b]	same/post 1797 rate[c]
−2.603	100.110	Simanganya C	SMY-C	−4.8 ± 2.7		30 (?)	>20						
−2.594	100.101	Simanganya A	SMY-A	−5.1 ± 0.5		3 ± 3	10 ± 5	>40 (30)	(30)	(0)	(90)	175 ± 27	same/post 1797 rate[c]
−2.752	99.995	Silabu	SLB							>25			
−2.726	100.213	Cimpungan A	CMP-A		−8.9 ± 1.3	10 ± 5	10 ± 5			0 ± 3	>22	70 ± 10	Singingi (SGG)[d]
−2.730	100.215	Cimpungan C	CMP-C	−4.8 ± 1.4									
−2.733	100.217	Cimpungan B	CMP-B					25 ± 5	36 ± 16				
−3.083	100.268	Bulasat	BLS	−10.7 ± 1.8		6 ± 3	5 ± 3	>52 (50)	(0)	(0)	(150)	237 ± 75	P. Pasir (PSR)[d]
−3.128	100.312	P. Saomang	SMG		−9.6 ± 2.0					0 ± 3	>10	99 ± 13	same
−3.213	100.460	P. Pecah Belah B	PCB-B	−3.0 ± 0.8	−7.9 ± 2.7	0 ± 5	15 ± 5	5 ± 5	5 ± 5	0 ± 3	>50	39 ± 9	same/P. Simaturugogo (STG)[e]
−3.288	100.454	P. Kumbang	KBG		−5.3 ± 0.6				3 ± 3	0 ± 3	>40	53 ± 7	same/Bangkaulu (BKL)[e]
−3.268	100.572	P. Simungguk	SGK								>10		
−3.486	100.638	P. Sanding A	SDG-A		−2.6 ± 1.0		>14	10 ± 3	20 ± 5		>35	35 ± 19	same

[a]Projected uplifts that are totals over multiple events (parenthetical numbers show best estimates for each event).
[b]Projected from 1833 and corrected for estimated 1797 uplift.
[c]Deformation rate before 1797 is assumed to be the same as after 1797.
[d]Both deformation rate and eighteenth-century absolute HLS inferred from a neighboring site.
[e]Eighteenth-century absolute HLS from the same site, deformation rate from a neighboring site.

a period of weeks or months [e.g., *Saji et al*., 1999]. However, we cannot completely rule out a tectonic cause. If tectonic, the uplift was centered on North Pagai and possibly extended to southern Sipora and most of South Pagai.

3.1.1.2. 1597

This event caused ~10 cm uplift throughout the Pagai Islands and up to 40 cm uplift on Sipora; there are no data to constrain whether it extended as far as Siberut. This relatively small uplift did not completely kill reefs at any site, so it was possible to directly measure the total uplift.

3.1.1.3. 1613 and 1631

These events form an interesting pair, both centered on the Pagai Islands and clearly terminating on southeastern Sipora. However, their trench-perpendicular uplift gradients slope in opposite directions, suggesting rupture of two megathrust patches updip and downdip from each other. The 1631 event is the only known case (including 1797, 1833, and 2007) with peak uplift along the northeastern coast of the islands rather than the southwestern coast, indicating that there was less shallow slip in 1631 than typically occurs. These relatively small uplifts (up to 50 cm) also did not completely kill reefs at most sites, so that total uplifts can be estimated based on measured minimum uplifts and totals at neighboring sites.

3.1.1.4. 1658 and 1703

The final events in the series were clearly much larger than their predecessors, completely killing reefs over significant areas. Reefs throughout Siberut were killed in 1658, and the paucity of data in that area dating to the following 1700s–1800s supercycle [see *Philibosian et al*., 2014] makes it impossible to estimate the total uplift by projecting interseismic rates backward in time. However, uplift decreased to the southeast across Sipora and clearly terminated between Sipora and the Pagai Islands. Uplift in 1703 was likely even larger, killing reefs throughout the Pagai Islands and Sipora. All of the total uplift measurements for 1703 are estimated by projecting interseismic deformation rates backward in time from the middle to late 1700s.

3.1.1.5. Comparisons to 1797 and 1833

For ease of comparison, we have reproduced uplift maps for 1797 and 1833 [from *Philibosian et al*., 2014] in Figure 12. Based on the analysis above, the 1703 uplift pattern is quite similar to the 1833 pattern, with peak uplift on the southwest coast of South Pagai, diminishing across North Pagai and Sipora, and likely terminating between Sipora and Siberut. As in 1833, the uplift may well have extended farther southeast of the islands, along strike. However, the uplift magnitudes of 1703 are about half the size of 1833 values in any given location.

While the 1597–1703 rupture sequence involved at least five discrete events, it appears that only the final two events were comparable to the 1797/1833 events. Deformation gradients for the earlier events were much less steep, while those for 1658 and 1703 were similar to those derived for 1797 and 1833 [*Philibosian et al*., 2014] and to those observed for recent Sunda megathrust ruptures [*Briggs et al*., 2006; *Sieh et al*., 2008]. Like the 1797/1833 pair, the 1658 and 1703 events were composed of a northwestern rupture followed by an overlapping southeastern rupture, but both were smaller than their analogs in the following supercycle culmination. The 1658 rupture clearly did not extend beneath the Pagai Islands, whereas the 1797 rupture definitely did, and while the extent of uplift was similar in 1703 and 1833, the uplift magnitude was about 50% smaller in 1703. We infer that the combination of the 1597, 1613, and 1631 events released a significant portion of the accumulated strain on the megathrust beneath Sipora and the Pagai Islands, resulting in a curtailed northwestern rupture and a lower magnitude southeastern rupture. Furthermore, at most sites total uplift for all events in the 1597–1703 series was substantially less than the combined 1797 and 1833 uplift. This difference is possibly related to reduced strain buildup beneath the central Mentawais during this supercycle, as discussed in the following section.

3.1.2. Interseismic Deformation

As we discovered was the case for the historical supercycle culmination of 1797–1833 [*Philibosian et al*., 2014], the periods before and during the 1597–1703 rupture sequence exhibit differing patterns of interseismic subsidence (Figure 13), and the change observed is similar to the 1797–1833 case. During the middle to late 1500s, prior to the first event in the rupture sequence, the gradient of subsidence was roughly perpendicular to the trench, as is typically expected for the interseismic period. This pattern is similar to those exhibited during the two analogous late-supercycle strain-accumulation periods of 1750–1797 and 1950–2007 [*Philibosian et al*., 2014].

In contrast, between 1597 and 1703, a more complex subsidence pattern emerged. Subsidence rates increased in the central Pagai Islands, but decreased farther northwest from the tip of North Pagai to southeast Sipora. These changes are revealed not only synoptically, in map view, but are also clear in records from

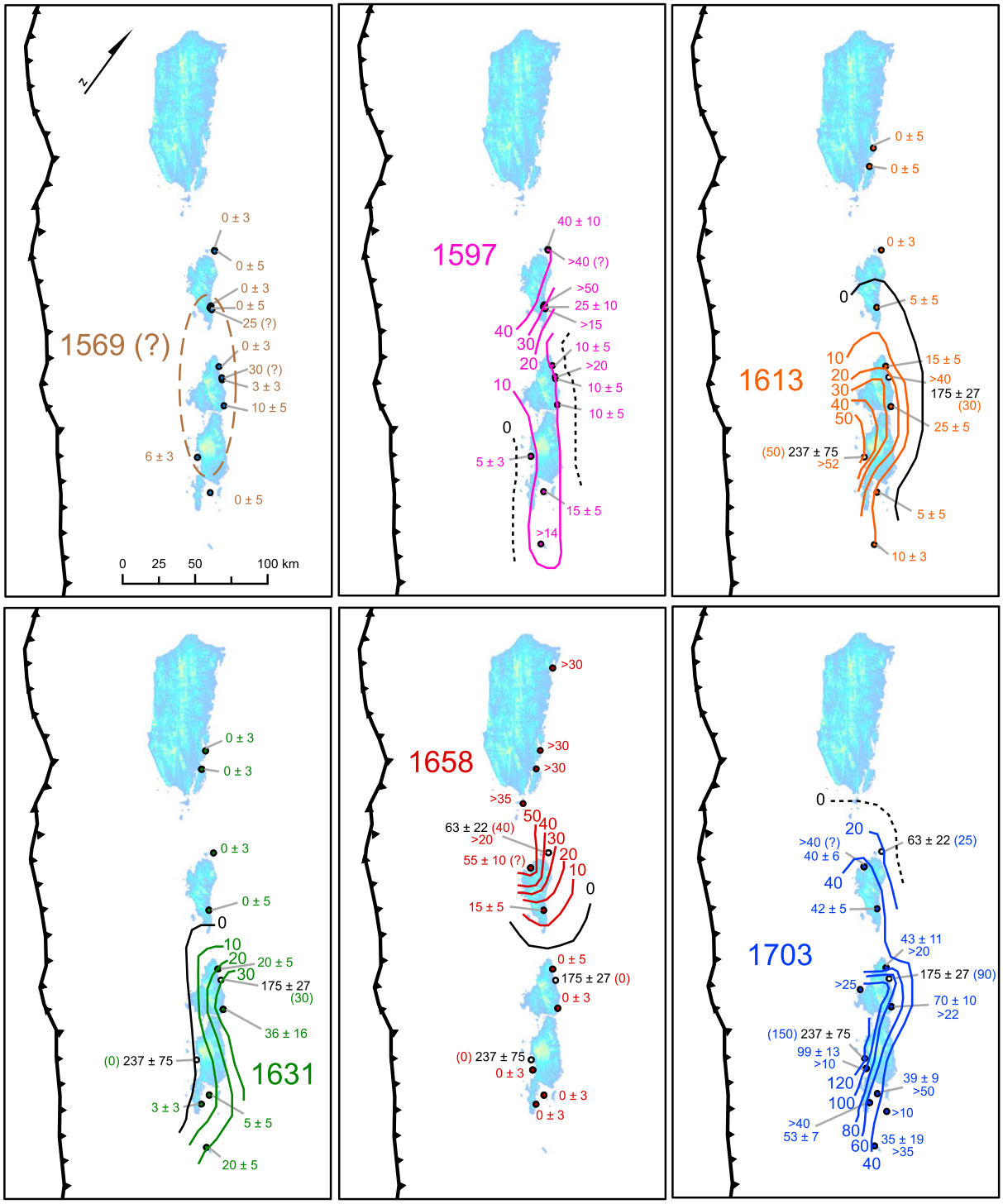

Figure 11. Contour maps of the five (possibly six) uplift events that form a rupture sequence spanning the seventeenth century. All measurements are in centimeters with 95% confidence intervals. Total uplifts for 1703 are calculated by projecting interseismic subsidence rates backward in time from younger coral records. The black numbers are totals over multiple events with colored numbers in parentheses indicating the estimates for each event. The 1703 event has a much steeper uplift gradient than the others; note that it is contoured at 20 cm intervals rather than 10 cm. Each event involves a different rupture area. Notably, the peak in uplift for the 1631 event is along the northeast rather than southwest coast of the islands, suggesting a rupture centered deeper on the subduction interface than commonly occurs.

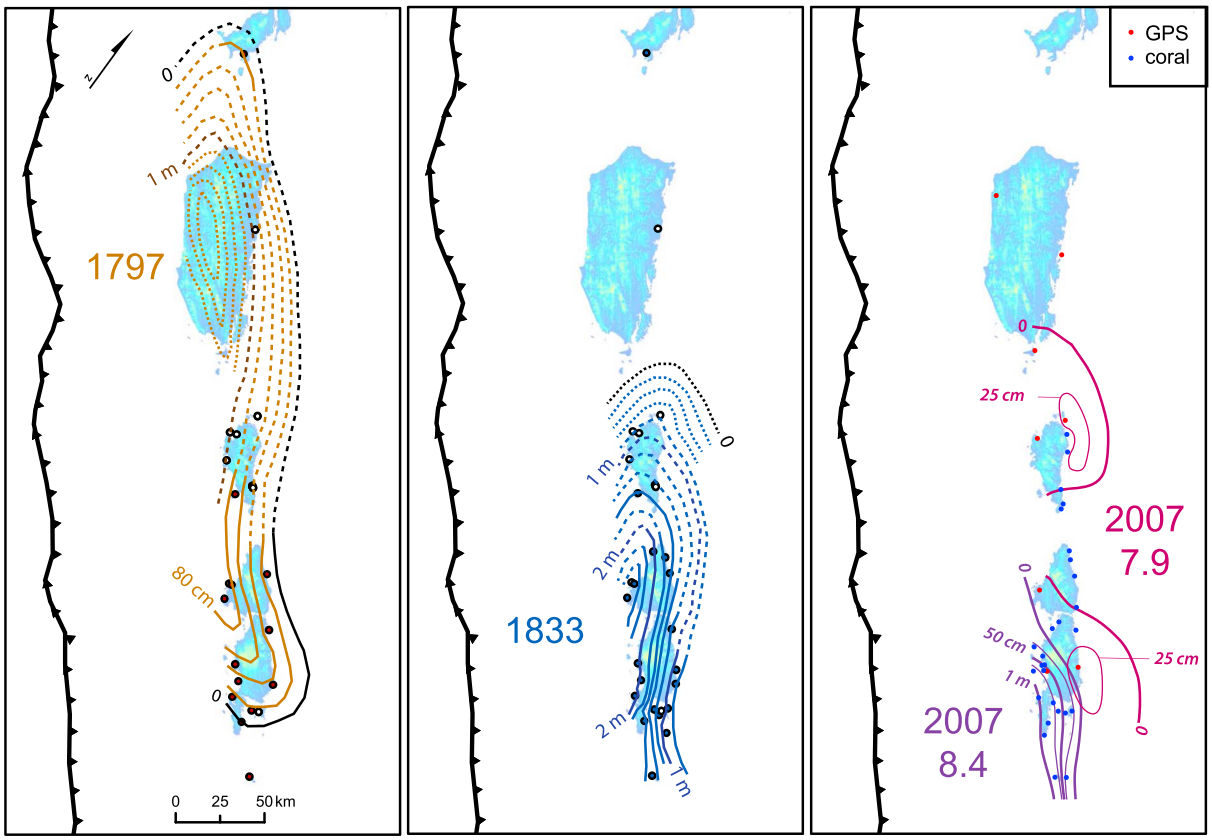

Figure 12. Coseismic uplift patterns of the great 1797, 1833, and 2007 earthquakes, simplified from *Philibosian et al*. [2014] and *Sieh et al*. [2008], for comparison to the 1600s rupture sequence. On the first two maps, the filled circles indicate sites where 1797 uplift could be determined separately from 1833 uplift. The empty circles indicate sites where reefs died completely in 1797, so the partitioning of uplift between the two earthquakes is uncertain. The dashed contours show inferred uplift at these sites based on likely uplift gradient and trends of more certain contours. The dotted contours are conjectural.

individual sites, most notably Sikici (Figure 10) [*Sieh et al*., 2008], Cimpungan (Figure 8), and P. Pecah Belah (Figure S15). Changes may also have occurred on Siberut and southeast of the Pagais, but are less clear due to the scarcity of data during one or both periods. The deformation pattern during the 1600s is similar to the analogous period between the great ruptures of 1797 and 1833 supercycle culmination period, but the changes from the prerupture period are slightly more pronounced in the 1600s case.

As in the 1797–1833 case, the change in deformation pattern presumably reflects changes in megathrust coupling triggered by the early events in the rupture sequence. In most of the records, it is difficult to discern exactly when the changes occurred because the 1597, 1613, and 1631 events are so closely spaced and coral growth rates must be averaged over decades to give robust tectonic deformation rates. However, in the Sikici records the 1613 and 1631 uplifts are negligible and the deformation rate clearly changed immediately after the 1597 uplift. Therefore, it is likely that the coupling pattern was altered by the first rupture in the series (1597).

As discussed by *Philibosian et al*. [2014], changes in submergence patterns may be confidently attributed to tectonic effects, whereas it is problematic to directly compare submergence rates from different time periods as they are affected by regional sea level changes. With that caveat in mind, we note that the submergence rates in most locations were generally ~2 mm/yr slower during the 1500s than during the two subsequent late-supercycle periods of 1750–1797 and 1950–2007. If the slower submergence rates during the 1500s do reflect tectonic effects rather than oceanographic effects, the megathrust coupling beneath the islands was weaker during the 1500s than during subsequent periods of strain accumulation. The reduced strain accumulation potentially explains why the total uplift in 1597–1703 was smaller than in 1797–1833.

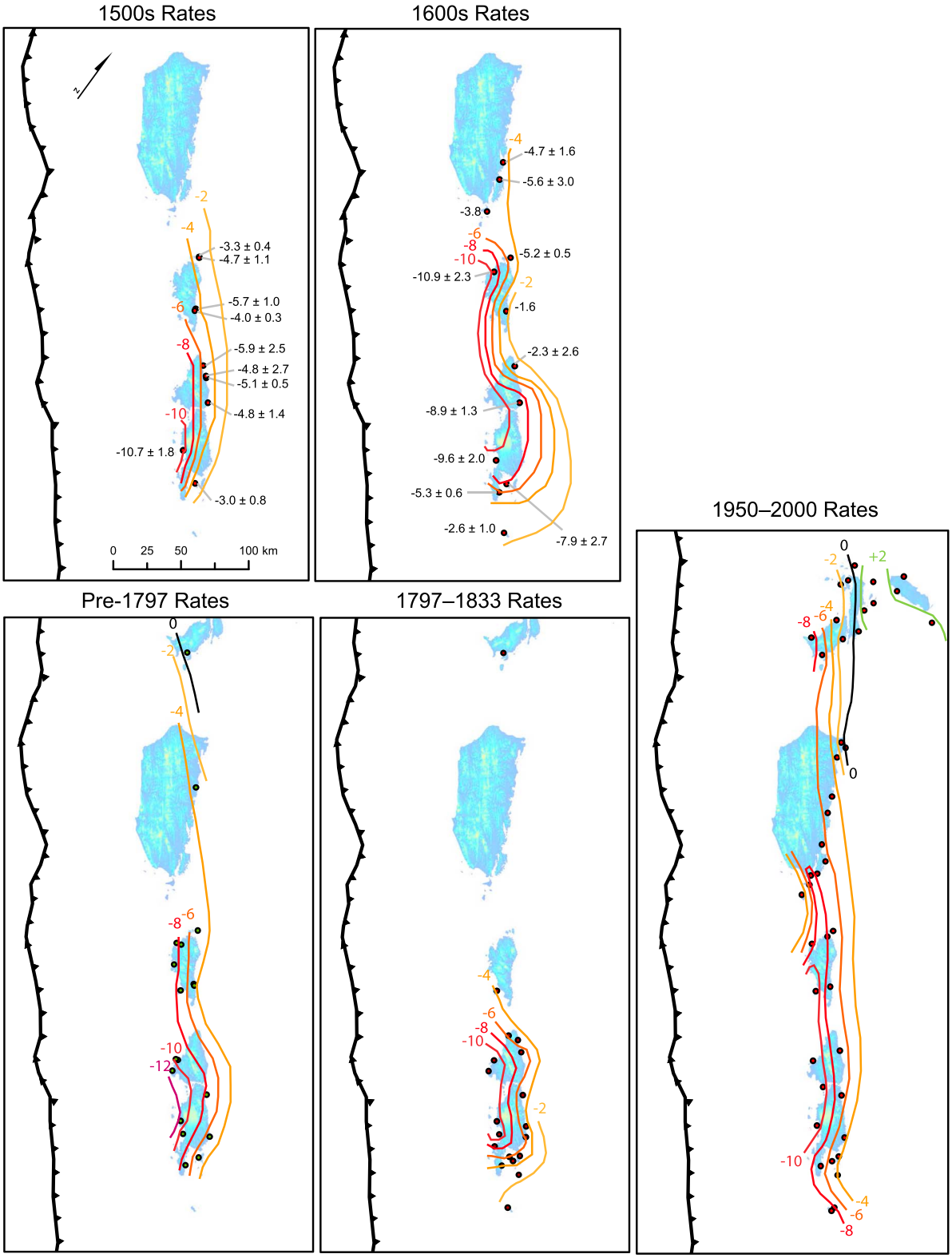

Figure 13. Contour maps of vertical interseismic deformation during the 1500s and 1600s, with simplified maps for more recent time periods from *Philibosian et al.* [2014] shown for comparison. All measurements are in mm/yr with 95% confidence intervals. Negative values indicate subsidence. The 1500s map includes all records before the ~1597 earthquake, while the 1600s map includes all records after that event. In the 1500s, near the end of a supercycle, before the first earthquake in the rupture sequence, the pattern reflects simple interseismic fault coupling with the gradient of subsidence roughly perpendicular to the trench. In the 1600s, between earthquakes, a more complex pattern emerged reflecting a more heterogeneous coupling state (similar to what occurred after the 1797 earthquake).

3.2. Fault Slip and Coupling Models

To relate the observed surface deformation to fault behavior at depth, we apply the same modeling procedure as *Philibosian et al.* [2014]. A detailed description of the assumptions, justifications, and citations can be found in that paper. In brief, we perform inverse modeling in an elastic half-space using the iterative version of the Principal Component Analysis Inversion Method (PCAIM), developed by *Kositsky and Avouac* [2010] and refined by *Perfettini and Avouac* [2014]. We model the megathrust as a curved fault plane made up of 15 × 15 km rectangular patches, starting at 1.2 km depth and 7.5° dip below the trench axis and ending at 100 km depth and 29° dip below the Sumatran coastline, a two-dimensional approximation of the Slab 1.0 model [*Hayes et al.*, 2012]. All models have a zero-slip or zero-coupling boundary condition along the lower edge of the model fault at 100 km depth, as this is likely the base of the seismogenic zone.

As the coral data provide only the vertical component of deformation, we cannot constrain the rake of slip on the megathrust, so all models are restricted to pure dip-slip motion. We regularize the underconstrained inversion problem by penalizing rough slip distributions via a Laplacian penalty term in the cost function; this factor is also spatially weighted depending on model resolution. In general, we apply the maximum amount of smoothing to the inversion that the data can bear until the misfit (reduced chi-square) sharply increases (see Figure S17). We relate megathrust slip to seismic moment using a shear modulus of 65 GPa, based on the average (down to 100 km depth) of the one-dimensional CRUST 2.0 layered structure model for this region [*Bassin et al.*, 2000].

3.2.1. Coseismic Models

Figure 14 shows megathrust slip models for each of the five inferred ruptures in the seventeenth-century sequence, along with slip models for 1797, 1833, and 2007 for comparison. The 1597, 1613, 1631, and 1658 uplift distributions can each be well fit by an M_w 8.1–8.3 earthquake rupture with large areas of slip between 1 and 2.5 m. The degree of concentration of the slip is largely a function of smoothing. To make the models more easily comparable we apply the same Laplacian penalty to all our coseismic models (the 1597, 1631, and 1658 models could be smoothed significantly more strongly without an appreciable increase in misfit; residuals are shown in Figures S18 and S21 and reduced chi-square values in Table S2).

As noted by *Philibosian et al.* [2014], vertical deformation measurements on the Mentawai Islands are largely insensitive to the behavior of the shallow megathrust (see coseismic model resolution maps in Figures S19 and S21). The shallow portion of the Mentawai segment is known to rupture seismically, individually during the 2010 tsunami earthquake [e.g., *Hill et al.*, 2012] and an ancient shallow event [*Philibosian et al.*, 2012], and likely in conjunction with the intermediate-depth seismogenic zone in 1797 and 1833, based on historical tsunami reports summarized by *Natawidjaja et al.* [2006]. The models in Figure 14 have a zero-slip boundary condition below the trench; models which are permitted to slip to the trench have slightly higher magnitudes and reproduce the data equally well (Figures S20 and S21).

Perhaps the most interesting feature of these models is that the first three events have broadly complementary slip distributions (Figure 15). Although there is some overlap, each event dominantly ruptures a different area and could probably be alternatively modeled with little or no overlap using weaker model smoothing. Summed together the 1597, 1613, and 1631 ruptures mosaic the whole megathrust beneath the Mentawai Islands. The 1658 event then re-ruptured the northwestern half of the segment and may have been significantly larger than the model shown here, as the measured uplifts on Siberut are merely minima. Finally, the 1703 earthquake re-ruptured the southeastern half of the segment. It was clearly larger than its predecessors, with a maximum slip of 5 m and a magnitude of at least 8.5. Given that the uplift magnitudes do not taper off to the southeast, it is likely that the 1613, 1631, 1703, and possibly 1597 rupture areas extended farther along strike in that direction, beyond the region constrained by our data (as did the 2007 M_w 8.4 rupture).

As suggested by the relative uplift distributions (see Figures 11 and 12), the modeled 1703 and 1833 slip areas are quite similar but the 1833 slip magnitude is nearly twice as large. The 1658 slip area is shorter along strike than 1797, and possibly lower magnitude as well (the magnitude of slip in 1658 below Siberut is a minimum). The 2007 event has similar slip magnitudes to 1703 but is shorter along strike than either 1703 or 1833.

We speculate, given these data, that the ongoing rupture sequence will probably evolve similarly to the seventeenth-century sequence, with several M_w 8–8.5 ruptures producing earthquakes and possibly tsunamis along different parts of the megathrust, rather than filling the remaining gaps in a single event.

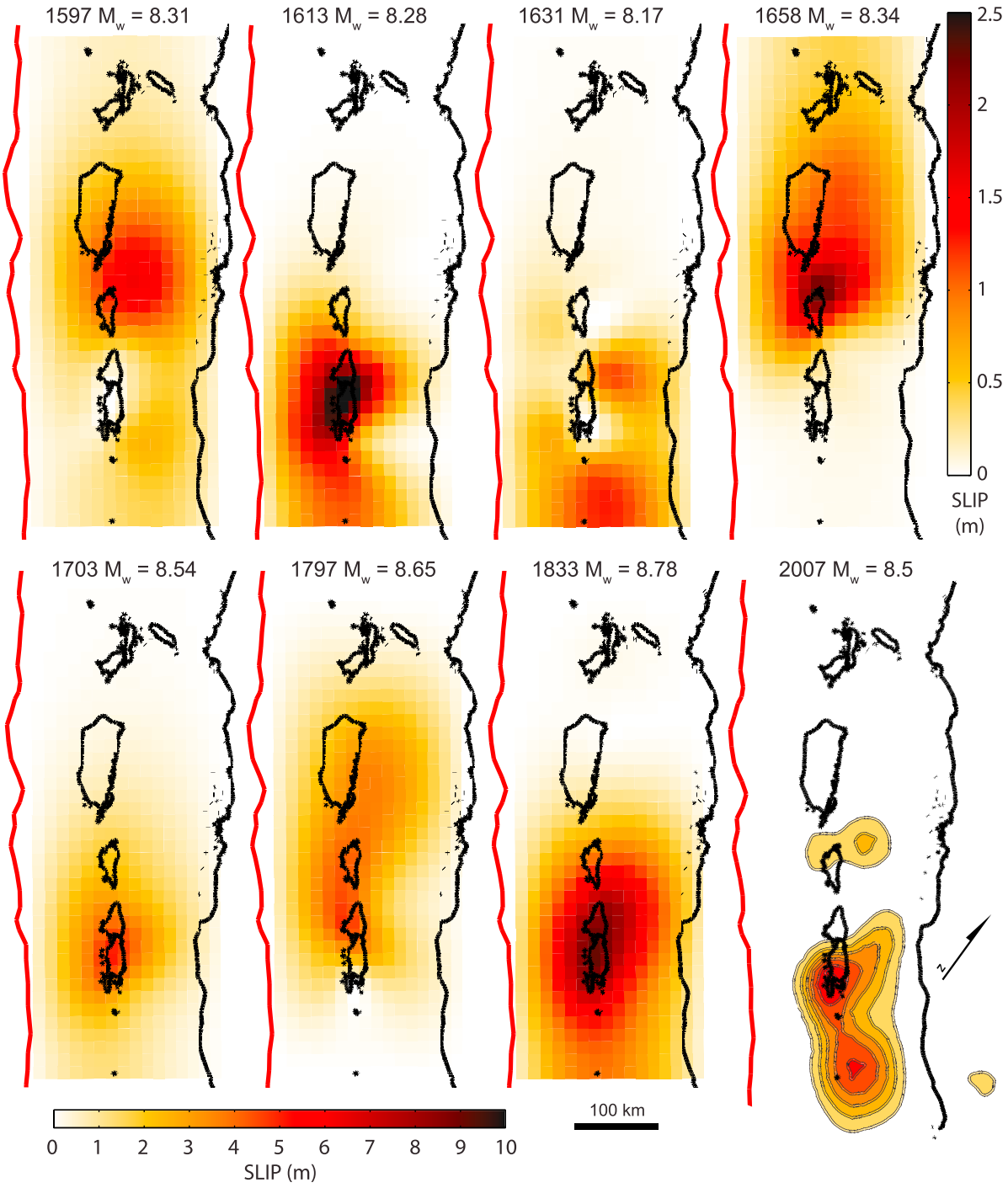

Figure 14. Models of coseismic fault slip for the 1597–1703 sequence. Slip in 1658 beneath Siberut may actually have been much larger; this model represents a minimum. Modeled slip distributions for the 1797 and 1833 earthquakes [from *Philibosian et al.*, 2014] and 2007 cluster [from *Konca et al.*, 2008] are shown for comparison. Note that the color scale maximum slip is 2.5 m for the top row and 10 m for the bottom row.

3.2.2. Interseismic Models

As in our previous paper [*Philibosian et al.*, 2014], we use a back slip formulation to relate interseismic deformation to megathrust coupling, with 100% coupling defined as back slip at the trench-perpendicular convergence rate of 45 mm/yr based on the regional model of Australia-Sunda subduction [*Chlieh et al.*, 2008]. We remove all coseismic offsets from the coral data set, further "clean" it by removing severely eroded points, and assign uncertainties of ±2.6 cm to preserved points and ±5 cm to moderately eroded points. We use a

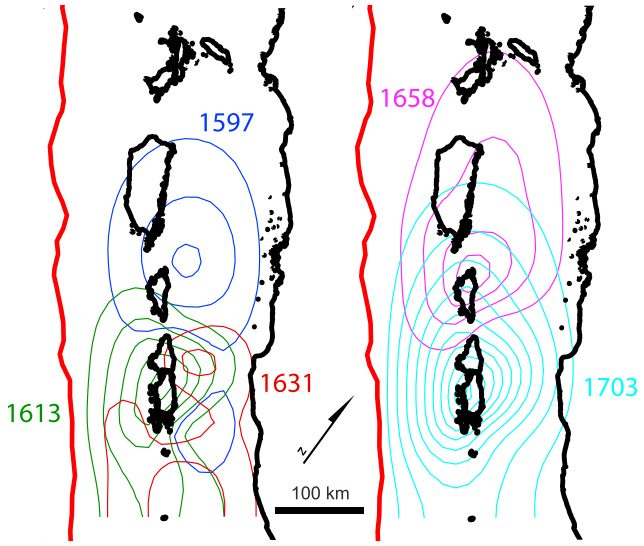

Figure 15. Slip contours of the 1597–1703 events, at 50 cm intervals starting at 50 cm. Note that the peak slip areas for the first three events are complementary, with each successive event filling in areas of zero or low slip in the previous patterns. The final two events re-ruptured the entire fault plane.

single time series for each site (a concatenation of the best-preserved coral records) and extrapolate synthetic data with ±10 mm/yr uncertainties to fill the entire time interval from 1520 to 1702, based on a linear fit to the real data. Thus, the distribution of sites and spatial model resolution (see Figure S22) is the same throughout the time period of interest, reducing spurious differences between models due to different spatial distributions of data.

PCAIM works by decomposing the data time series into temporal (*V*) and spatial deformation (*U*) eigenvectors, inverting the U eigenvectors to obtain corresponding fault slip eigenvectors (*L*), and recombining *L* and *V* to produce a complete time series of fault slip. To first order, the interseismic deformation clearly has a linear time function, so we impose linearity on the first time component while allowing the second component to remain free (including additional principal components did not provide a significantly better fit). Thus, the second component highlights deviations from linearity.

Eigenvectors for a model of the full 1520–1702 time period (Figure 16) reveal a fairly typical coupling pattern for the first (linear) component, and a more complex pattern for the second (free) component. The free time function V_2 clearly illuminates three epochs with distinct behavior: a moderate positive trend from 1520 to 1580, a steeply negative trend from 1580 to 1650, and a steeply positive trend from 1650 to 1702. Though defined purely based on the observed trends in V_2, these epochs probably represent different supercycle stages. The first epoch spans the late-interseismic period leading up to the 1597 earthquake, the second encompasses the first three closely-spaced earthquakes in the rupture cascade, and the third includes the 1658 earthquake and leads up to the final 1703 earthquake. However, simultaneously modeling the entire period of interest produces un-physical or unlikely results during certain intervals, such as greater than 100% coupling and patches of afterslip adjacent to patches of strong coupling. In the PCAIM process it is difficult to enforce constraints on subsets of the full time period, so we instead model the three time periods individually (each with a linear and free component). Components and time series for these models are shown in Figures S23–S28 and reduced chi-square values in Table S3. As with the coseismic models, we apply the same weight of Laplacian smoothing to all three interseismic models, based on the 1580–1650 period which can tolerate the least smoothing (see Figure S17).

The individual models (Figure 17) reveal substantial differences in coupling pattern among the three time periods. The late-supercycle period of 1520–1580 exhibits coupling downdip of the islands, with significant along-strike variations. There are notably similar features to the other late-supercycle periods of 1755–1797 and 1950–2000, such as the strongest coupling centered beneath the Pagai Islands and a trough in coupling in the vicinity of Sipora Island [*Philibosian et al*., 2014]. However, as discussed above, the submergence rates in the late 1500s were slower than during subsequent late-supercycle periods, and this is reflected in a generally lower degree of modeled coupling.

During the intermediate 1580–1650 period, coupling apparently migrated updip of the Pagai Islands. This reflects reduced submergence rates at many sites during this period. It is important to note that due to the close temporal spacing of uplift events during this period, it is difficult to accurately estimate the submergence rates between uplifts. Due to oceanographic noise, coral-based deformation rates are best averaged over decades, and the precise details of the record are often obscured by erosion, especially in the temporal vicinity of uplifts which leave corals exposed to wave action. If the true coseismic uplift is underestimated due

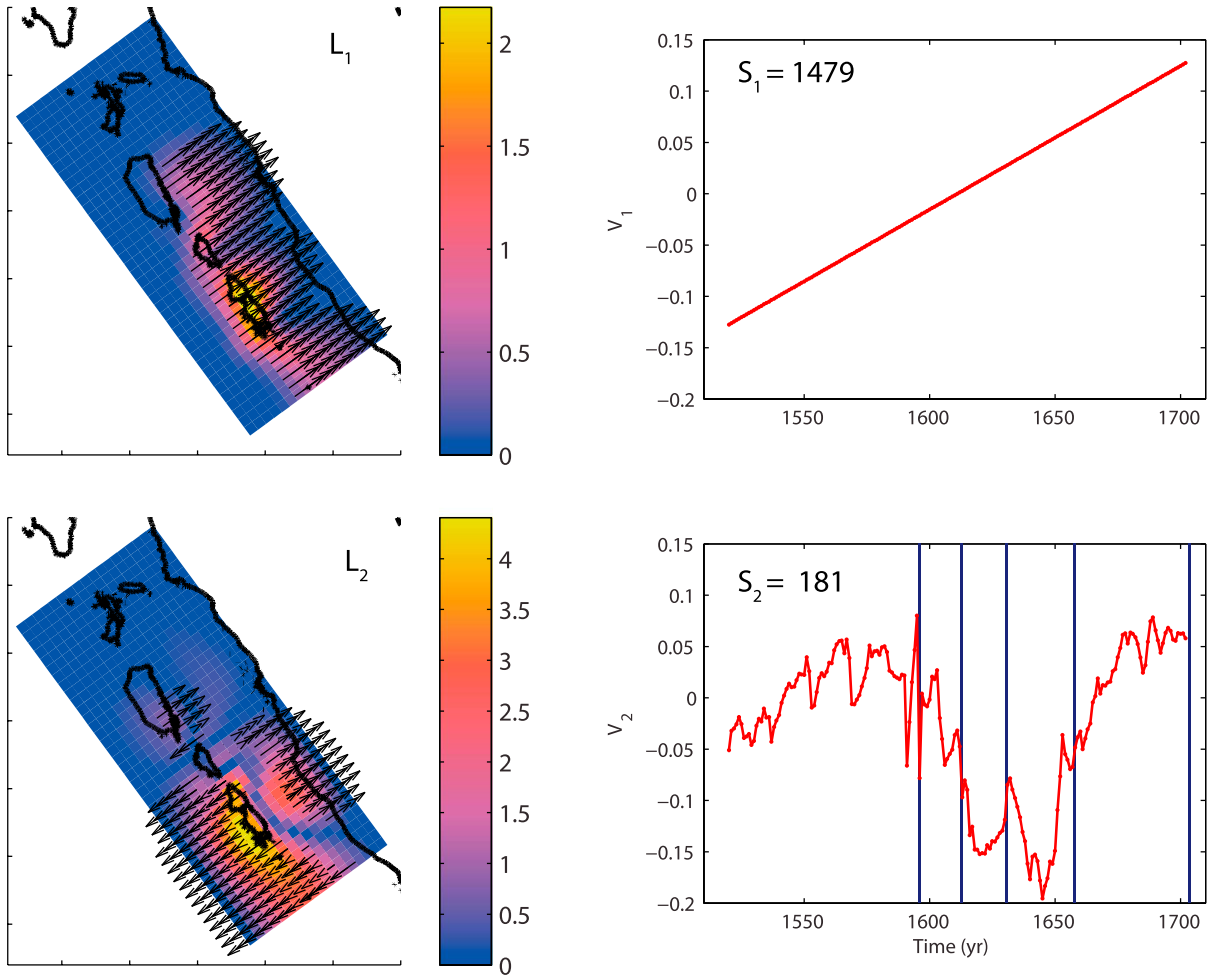

Figure 16. Spatial (*L*) and temporal (*V*) eigenvectors for a two-component model of interseismic deformation from 1520 to 1702 (coseismic offsets removed). Eigenvectors are normalized; eigenvalues (*S*) indicate the relative magnitude of the components. V_1 is imposed as a linear time function and corresponds to a typical coupling pattern; V_2 is a free component which represents deviations from linearity. Amid high-frequency noise that is related to oceanographic fluctuation, three distinct episodes are evident in the second component: a moderately positive trend from 1520 to 1580, a steeply negative trend from 1580 to 1650, and a steeply positive trend from 1650 to 1702. For reference, the vertical blue lines indicate earthquake years.

to erosion, a part of the coseismic uplift remains in the data and will appear as a reduced interseismic subsidence rate. Due to this ambiguity, it is difficult to confidently interpret the coupling behavior during the 1580–1650 interval.

During the final 1650–1702 period, leading up to the final event in the rupture sequence, coupling was again centered downdip of the islands, but there are many notable differences from the prerupture 1520–1580 period. Coupling downdip of Sipora and South Pagai markedly increased, while it decreased beneath North Pagai and Sanding. Patches of coupling also appeared updip of the latter two areas, a reflection of the extremely slow submergence rates in those areas. While there are undoubtedly other coupling distributions which could reproduce the data, there is no way to do so without a major change between the prerupture period and the inter-rupture period, including coupling distributions that are heterogeneous at the ~50 km scale. As we found in the 1797/1833 case [*Philibosian et al.*, 2014], the fault patches beneath the central Mentawais and Sanding Island behave capriciously, changing their coupling patterns after ruptures and often serving as rupture termini, whereas the South Pagai asperity has the relatively constant behavior of remaining strongly coupled, both before and during the rupture sequence.

We have made a visual representation of the complete interseismic and coseismic megathrust slip from 1520–1703 in the supplemental animation (Movie S1 in the supporting information). The red and blue areas represent slip deficit and excess, respectively, relative to the assumed plate rate of 4.5 cm/yr of slip starting in 1520.

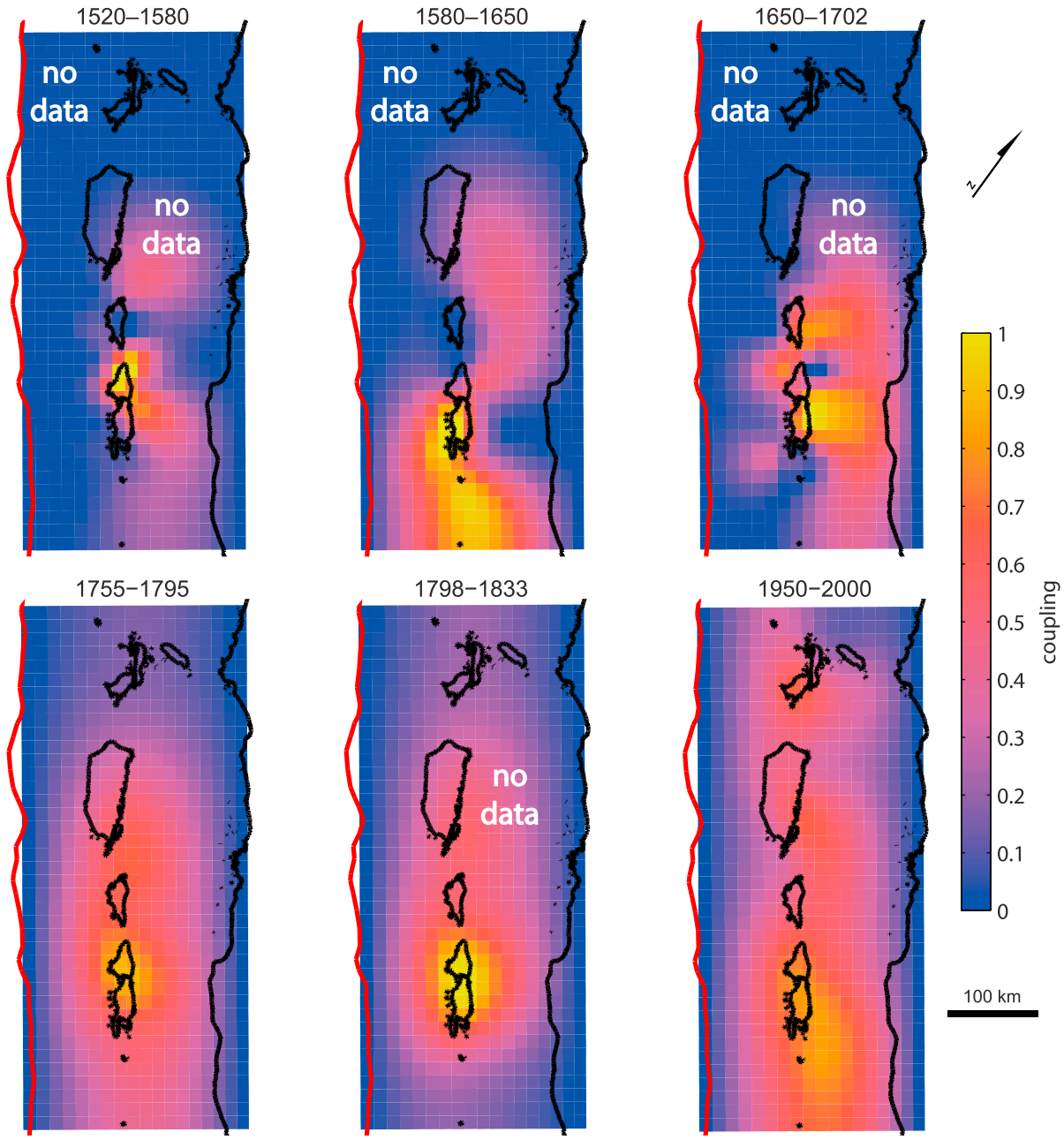

Figure 17. (top row) Separate interseismic coupling models for the three time intervals identified based on the decomposition of the full 1520–1702 period. The coupling pattern was substantially different during each of the three intervals. Note that the coupling pattern beneath Siberut is not constrained except during the early 1600s and is simply assumed to have been similar during the other periods. Coupling beneath the Batu Islands is not constrained at any time during the sixteenth or seventeenth centuries. (bottom row) For comparison, models of interseismic coupling during the three more recent time intervals for which widespread coral data exists [from *Philibosian et al.*, 2014].

4. Supercycles Before A.D. 1500

Coral microatolls recording deformation prior to 1500 are far more rarely preserved, with only a few sites representing each event (Figure 18). Maps of new sites and interpreted microatoll cross sections appear in Figures S29–S34, and a synthesis of previously published records of corals that died in the late 1300s appears in Figure S35. The data are insufficient to characterize the rupture sequences and interseismic periods as fully as we have done for the 1797/1833 and sixteenth- to seventeenth-century cases. Nevertheless, examining these data reveals familiar patterns, suggesting that many of the features and behaviors we identified in our analyses of the more recent supercycles are applicable to the longer term.

Figure 19 compiles all Mentawai coral records dating between A.D. 1 and 1500, shifted within their age uncertainties based on likely correlations between records. The persistence of the supercycle pattern is evident, with groups of events typically spanning several decades separated from each other by 100–200 year interseismic periods. Even with these incomplete data, it is possible to compare and contrast these earlier supercycles with their successors.

As noted by *Sieh et al*. [2008], a rupture circa 1350 recorded by several South Pagai sites clearly did not significantly uplift North Pagai and Sipora, while the following rupture ~40 years later did uplift those areas. (We assign a more precise age of 1388 to the later event based on correlation of oceanographic die-downs, see Figure S35.) The ~40 year spacing between northwestern and southeastern large ruptures appears to be a common feature, although the order in which they occur varies (southeastern first in the 1300s and 2007; northwestern first in the 1500s–1600s and 1797). The 1300s sequence also features a rupture terminus beneath the central Mentawais, but it is unclear whether the ~1350 and ~1388 rupture areas overlapped. There is an intriguing hint of a decrease in subsidence rate around 1350 in the coral records from Sikici and Simanganya (see Figure S35). However, the highest parts of these microatolls are eroded and it is impossible to pinpoint exactly when the ~1350 event occurred in these records, as there was no uplift in ~1350 at these sites. Therefore, it is possible that the ~1350 event also triggered changes in coupling, but we cannot make a strong conclusion on that point. It is clear from the exceptionally long, continuous Pulau Pasir record [see *Philibosian et al*., 2012] that no significant uplifts occurred at that site for a century prior to 1350. The early part of that record suggests two uplift events 30 years apart in the early 1200s, perhaps part of the preceding rupture sequence, but we have no other microatolls of this age with which to correlate.

Stepping backward in time, three hat-shaped corals at Basua site B each record two large uplift events separated by several decades, but they are not necessarily correlative. If the ages are accurate, B1 recorded a pair separated by 30 years in the mid-700 s and B4 recorded a different pair separated by ~45 years in the late 700s to mid-800s (with a third, smaller intervening uplift). B2 potentially correlates with B4 but has a large age uncertainty and could potentially record a still different, younger pair of events separated by ~40 years. In each case, the two ruptures must have overlapped beneath South Pagai, although their extents are otherwise unconstrained. The records are not long enough to judge whether there were any changes in interseismic rate. Along with an eleventh-century chiseled sample from Silabu (NP94A6 [*Zachariasen*, 1998]), these are the only microatolls we have found whose ages lie within a long preservation hiatus between A.D. 700 and 1200.

The combination of relatively precisely dated corals at Silogui (Siberut) and Silabusabeu (North Pagai) reveals four distinct events between A.D. 520 and 700, the first two separated by only 4 years. Other fossil coral populations at Teleleu (Siberut), Bulasat (S. Pagai), and Basua B likely correlate with this sequence, but since their large age uncertainties each encompass multiple events, we cannot determine the precise chronology. At least three of the events overlapped beneath North Pagai since they are all recorded at Silabusabeu, and the corals at that site also record a clear change in interseismic rate after the 523/527 doublet.

A still earlier event around A.D. 400 is suggested by microatolls at Bulasat and Sibelua on South Pagai, preceded by at least a century of interseismic subsidence. For corals that predate A.D. 300, the frequency of microatoll preservation drops off significantly (older samples are summarized by *Philibosian et al*. [2012]).

All the records in Figure 19 support the conclusions that individual major ruptures typically involve either the northwestern or southeastern Mentawai segment (but not the full segment), that ruptures often overlap below the central Mentawais, and that ruptures typically occur in clusters that cumulatively cover the entire Mentawai segment at the culmination of each supercycle.

5. Long-Term Deformation Trends

One other feature of the Mentawai seismic cycle that bears revisiting is potential long-term or permanent vertical deformation. *Sieh et al*. [2008] noted that their three featured sites (Sikici, Simanganya, and Bulasat/Saomang) appeared to display long-term uplift over the three supercycles in their coral history (i.e., each generation of corals grew at a lower elevation than the previous generation). These trends suggested a long-term uplift rate of 1.8 mm/yr, although the fits to the data were not perfect. Having re-analyzed the coral data at those original three sites, added a fourth site that spans three supercycles, and added many

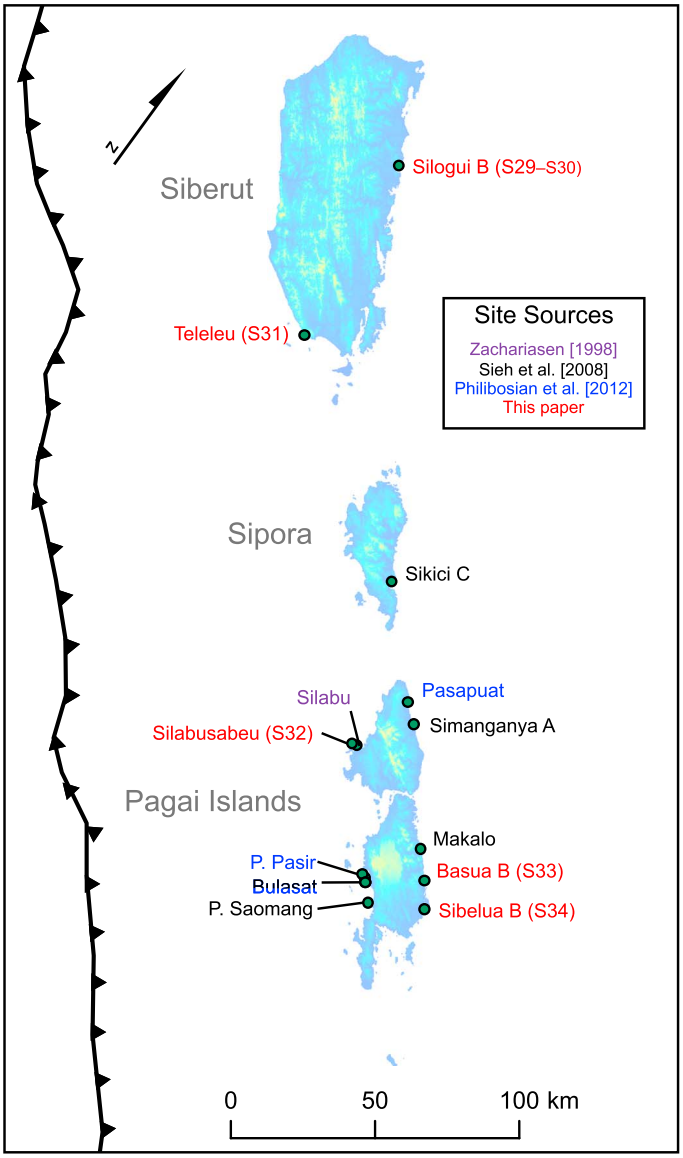

Figure 18. Locations of sites with coral microatoll data between A.D. 1 and 1500.

new sites that span two supercycles, we are now in a better position to accurately assess long-term vertical deformation.

Simplified "sawtooth curves" for all sites that have coral HLS elevation data in the 1600s are compiled in Figure 20. Records from the 1300s are included where available. These HLS records are shown by solid lines where constrained by coral at that site, and by dashed lines where inferred (gaps are filled by extrapolating known interseismic deformation rates and/or comparing with data from nearby sites). The records from Siberut, northernmost Sipora, and Sanding Island do not show significant evidence for long-term deformation (microatolls that died in the 1600s are found at similar elevations to modern microatolls). Most of the records from the rest of Sipora and the Pagai Islands (the central Mentawais) are at least roughly consistent with long-term uplift at rates between 1.4 and 2.8 mm/yr, and thin brown lines illustrating these potential trends have been added to those records. However, since each generation of corals provides only one data point, only those records that extend back to the 1300s can reasonably be used to argue strongly for such a trend. Of those, Bulasat/P. Pasir, Saomang, and Simanganya do strongly support these trends. Sikici is moderately supportive: the trend fits through the 1600s rupture sequence but the older 1300s data fall well below the projected elevation. *Sieh et al.* [2008] postulated that these older corals could have settled into the

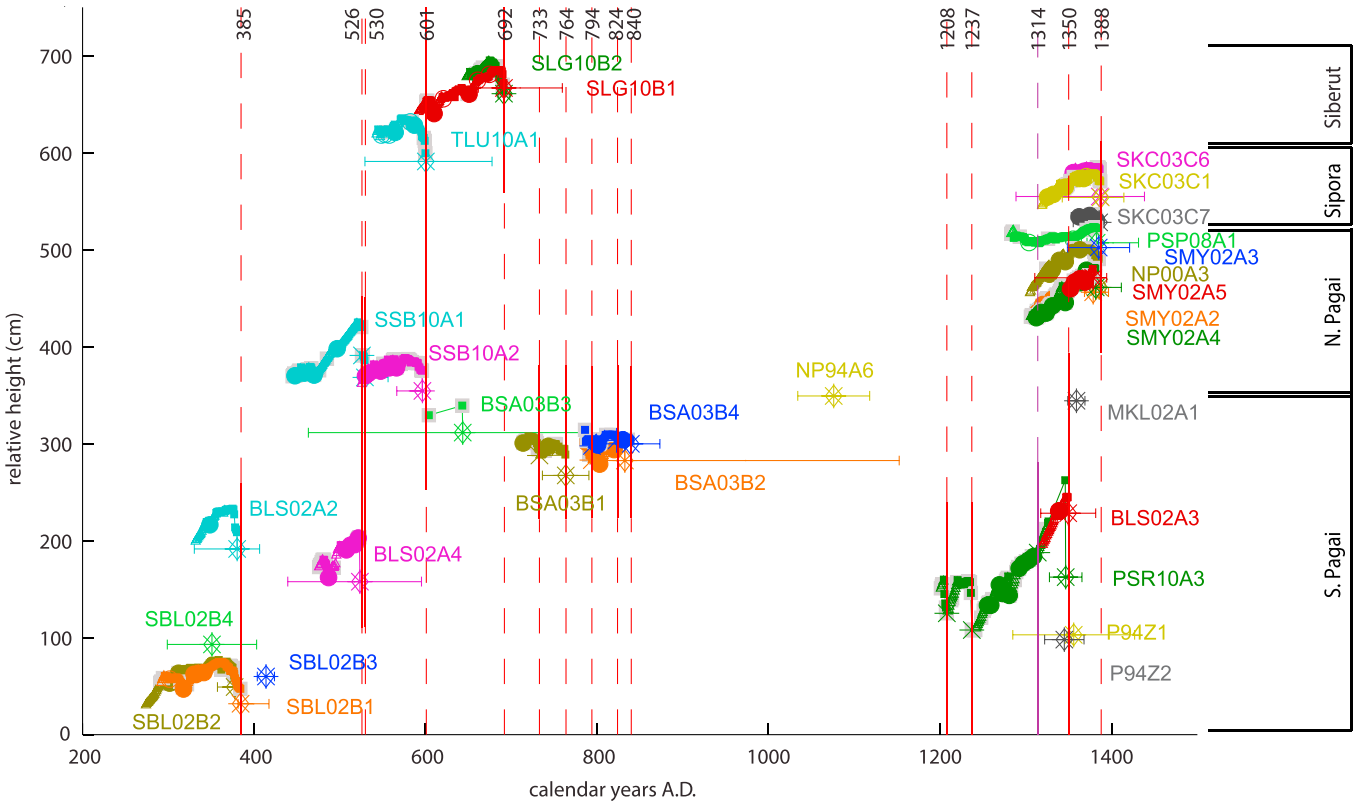

Figure 19. All Mentawai coral records dating between A.D. 1 and 1500, with sites ordered from NW to SE and each site vertically offset from the next (symbols as in Figure 11). The red vertical lines indicate dates of probable megathrust earthquakes based on coral uplift events (the circa1314 submergence event, a proposed shallow megathrust rupture, is shown with a purple line). Lines are dashed where uplift is small or unconstrained. Site abbreviations: SLG: Silogui, TLU: Teleleu, SKC: Sikici, PSP: Pasapuat, SMY and NP00A: Simanganya, SSB: Silabusabeu, NP94A: Silabu, MKL: Makalo, BSA: Basua, PSR: Pulau Pasir, BLS: Bulasat, P94Z: Saomang, SBL: Sibelua.

substrate, but this was largely a post hoc argument and the ~1 m of settling required would be extreme. The final site, Pasapuat, does not fit a constant long-term uplift trend at all (dashed trend line shown for reference only). Although all three generations of fossil microatolls are higher than modern ones, the fossil microatolls are all roughly the same elevation. At the majority of sites, which lack data from the 1300s, it is difficult to confidently distinguish between a Pasapuat-like history and a Simanganya-like history. In summary, there is moderate to strong evidence of slow long-term uplift over multiple supercycles throughout the central Mentawais, but zero long-term deformation farther northwest or southeast.

In a previous paper, we demonstrated that these long-term trends cannot represent permanent, inelastic uplift of the Mentawai Islands because microatolls thousands of years old are still found in the intertidal zone throughout the Mentawais [*Philibosian et al.*, 2012]. Sea level in this region is generally modeled and measured to have been slowly falling or steady over the last few thousand years [e.g., *Briggs et al.*, 2008; *Horton et al.*, 2005], so permanent uplift rates >0.2 mm/yr are largely precluded by those data. Remnants of reefs from the mid-Holocene sea level highstand are not as prevalent in the Mentawai Islands as they are on neighboring Nias Island [*Briggs et al.*, 2008], suggesting that if anything there has been net subsidence over the Holocene. We argued that the long-term uplift observed at Bulasat/P. Pasir was instead a manifestation of elastic strain accumulation on the shallow megathrust, periodically released in earthquakes such as the 2010 Pagai Islands earthquake and a circa 1314 shallow rupture [*Philibosian et al.*, 2012]. This likely millennial cycle of slow uplift and sudden subsidence appeared to be superimposed on the ~200 year cycle originating from the intermediate-depth megathrust interface. One possible explanation of the data in Figure 20 is that strain accumulation on the shallow megathrust over many supercycles similarly affects numerous sites throughout the central Mentawais but does not extend northwestward to Siberut or southeastward to Sanding. The data are too sparse and rates too poorly constrained to attempt any more detailed analysis or draw more solid conclusions.

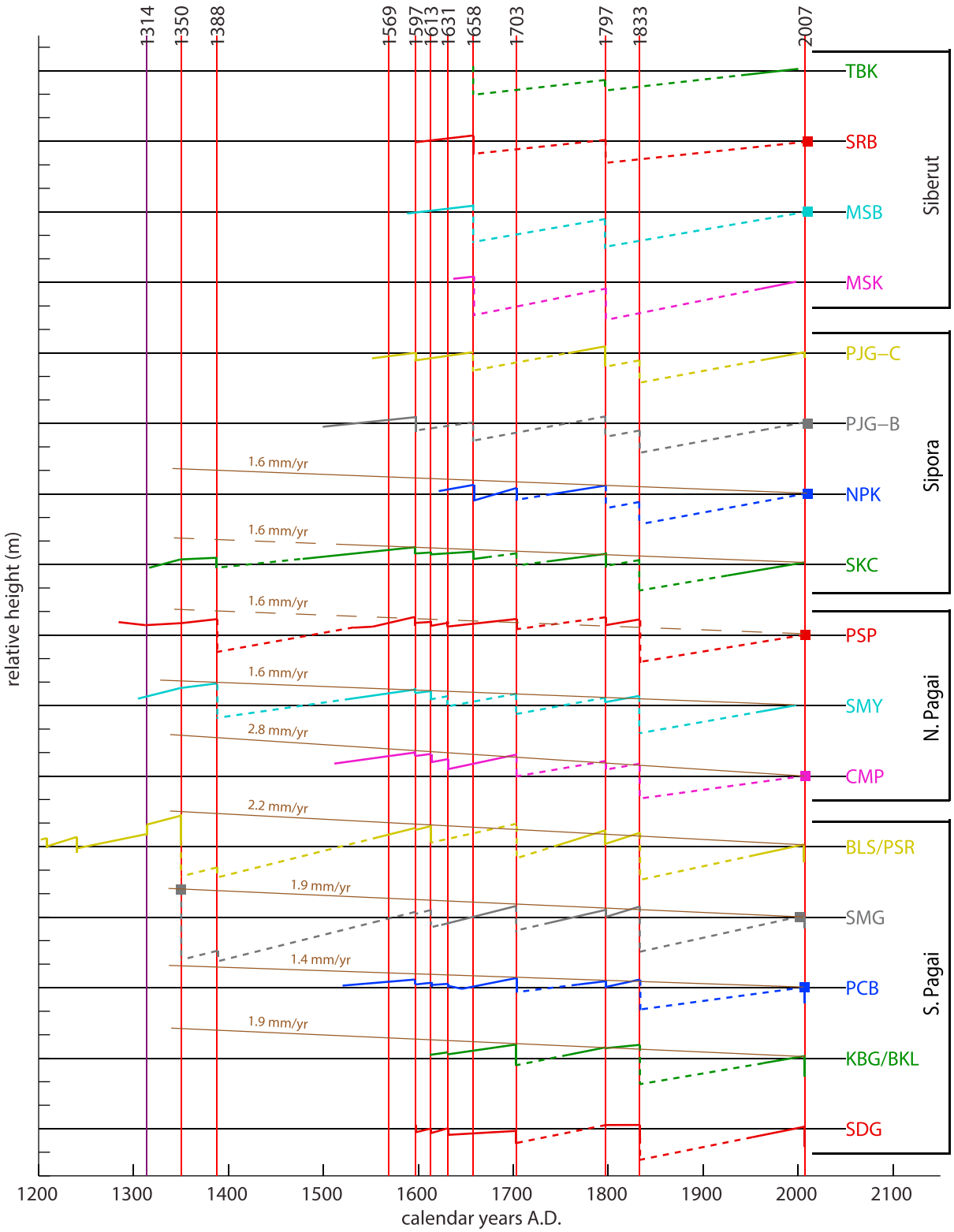

Figure 20. Sawtooth curves for all sites that have coral elevation data in the 1600s, extended to include 1300s data where available, ordered from northwest to southeast. In two cases, data from two sites a few kilometers apart have been combined into a single record. Each horizontal black line marks the zero elevation datum (HLS prior to 2007 earthquake) for that site. The colored lines represent simplified HLS histories at each site (solid where constrained, dashed where inferred). The colored squares indicate point measurements of HLS. The vertical lines mark dates of (likely coseismic) uplift and subsidence events. The brown lines and numbers indicate possible long-term uplift rates that have persisted over multiple supercycles (dashed where the fit to the data is not good).

6. Conclusions

Our analysis of Mentawai segment ruptures over the past millennium has revealed a great deal of variability: each supercycle evolves uniquely as various megathrust asperities rupture in different combinations. Each of the eight major ruptures we have analyzed (see Figure 14) has distinctive rupture extents and/or slip magnitudes. There does not appear to be a "characteristic earthquake" associated with any part of the Mentawai segment. Nevertheless, it is possible to identify common characteristics and "rules" that are relevant to fault behavior science and useful for seismic hazard analysis. While we do not have data from enough earthquake cycles to do a rigorous statistical analysis, we can form reasonable expectations based on the logic that a continuation of the type of behavior seen in all of our observations is more likely than a major departure from that behavior.

Failure in a sequence of partial ruptures is clearly a persistent feature of the Mentawai segment. We find no evidence of an end-to-end Mentawai segment rupture at any time in the past (though of course we cannot confidently state that it has never occurred). Every known supercycle culmination involves at least two events, one centered in the northwest and one in the southeast, generally overlapping beneath the central Mentawais by 100 to 200 km along strike. Most ruptures terminate somewhere between the archipelago south of Siberut and the strait between the Pagai Islands. Spatially and even temporally varying frictional properties of the megathrust beneath the central Mentawai Islands are likely responsible for these phenomena, producing the supercycle behavior. While there is likely a local rheological or structural reason for this heterogeneity, the observed variability in asperity grouping suggests that evolution of a given rupture cascade is significantly influenced by the extent and magnitude of the first rupture in the sequence and the changes in loading rate distribution that it triggers due to postseismic relaxation and altered interseismic coupling. Changes in interseismic coupling could result from pore pressure and temperature variations induced by the earthquake sequence through compaction/dilatancy effects and shear heating.

While we cannot say exactly how the ongoing rupture sequence will evolve, the sixteenth- to seventeenth century rupture sequence is probably a better analog for behavior over the next several decades than the 1797/1833 doublet. The 2007 M_w 8.4 rupture had a significantly smaller rupture area and slip magnitude than the 1833 rupture, indicating that there may be an additional southeastern rupture as well as the expected future northwestern rupture. The smaller 2007 M_w 7.9 and 2008 M_w 7.2 events ruptured individual asperities geographically separated from the M_w 8.4 rupture area [*Konca et al.*, 2008; *Salman et al.*, 2014]. If the 1597-1613-1631 sequence is any guide, future smaller ruptures may fill in the gaps to fully mosaic the megathrust. However, as illustrated by the 1658 and 1703 events that followed, re-rupture of individual asperities in larger events is also possible and even probable. Thus, the rupture areas of the 2007 and 2008 earthquakes should not be excluded from possible future rupture scenarios.

Defining a recurrence interval for a fault with supercycle behavior is challenging. It is not clear whether it would be more meaningful to measure the intervals between events that started rupture sequences (~250, ~200, and 210 years, the least variable interval) or between events that ended rupture sequences (~315, ~130, and 183+ years). There is significant variation in the duration of the purely interseismic periods between rupture sequences (~210, ~95, and 174 years). Furthermore, we cannot calculate statistically significant average periods or rigorously assess variability based on only three complete cycles (the chronology of past ruptures is almost certainly incomplete prior to 1350).

However, we can make a general statement that rupture cascades on the Mentawai segment occur approximately every 200 years. It is also interesting to note that the two largest events in each sequence have been separated by about 40 years in all three known cases (1350/1388, 1658/1703, and 1797/1833) and that the intervals between other events during the 1500s and 1600s were all less than 40 years. Based on these observations, we speculate that the next event in the ongoing rupture sequence will occur no later than the year 2047, though that event may not complete the rupture cascade (the sixteenth- to seventeenth-century cascade spanned ~105 years).

The uniquely detailed paleogeodetic records of the Sumatran portion of the Sunda megathrust provide an opportunity to characterize fault behaviors that are probably common but difficult to observe with other techniques. As we observed in the conclusion of our previous paper, there is evidence for supercycles culminating in rupture cascades on other megathrust faults (most notably parts of the South American subduction zone) and even on continental faults [*Philibosian et al.*, 2014, and references therein]. Coupling

changes triggered by earthquakes have been less commonly observed, but this is not surprising since the detailed geodetic records necessary to observe them are generally limited to the instrumental era. Several years of data before and at least a decade of data after an earthquake are required to positively identify such changes. Deformation rates throughout the Mentawai Islands did indeed change after the 2007 earthquakes [*Feng et al.*, 2015], but less than a decade after the earthquake it is still somewhat difficult to discern static rate changes amid the numerous decaying postseismic deformation transients. It remains to be seen whether our paleoseismology-based expectations for the ongoing Mentawai rupture cascade will be borne out, and whether Mentawai-style supercycle behavior will indeed prove a useful model for other fault systems around the world.

Acknowledgments

All data used in this paper are included in the main text or supporting information. This project was supported by National Science Foundation grants 0208508, 0530899, 0538333, and 0809223 to K.S.; by Sumatran Paleoseismology grant M58B50074.706022; by the National Research Foundation Singapore and the Singapore Ministry of Education under the Research Centres of Excellence initiative through the Earth Observatory of Singapore; by the Research Center for Geotechnology at the Indonesian Institute of Sciences (LIPI); by the Caltech Tectonics Observatory; and by the Gordon and Betty Moore Foundation. Also, the Japanese documentary agency NHK funded a special one-week final field expedition in 2012. U-Th dating was supported by the Taiwan ROC MOST and NTU grants 104-2119-M-002-003, 105-2119-M-002-001, and 105R7625 to C.-C. S. We thank Dudi Prayudi, Imam Suprihanto, John Galetzka, and all the crew members of the *K.M. Andalas* for field support, Ke (Coco) Lin for assistance with U-Th dating at the HISPEC Laboratory at the National Taiwan University, and Aron Meltzner, Emma Hill, and Lujia Feng for helpful discussions. This paper was improved thanks to thoughtful and thorough reviews by Rob Witter and an anonymous reviewer. This is Earth Observatory of Singapore contribution no. 137 and Caltech Tectonics Observatory contribution 216.

References

Abram, N. J., M. K. Gagan, M. T. McCulloch, J. Chappell, and W. S. Hantoro (2003), Coral reef death during the 1997 Indian Ocean Dipole linked to Indonesian wildfires, *Science*, *301*, 952–955.

Bassin, C., G. Laske, and G. Masters (2000), The current limits of resolution for surface wave tomography in North America, *Eos Trans. AGU*, 81 (48), Fall Meet. Suppl., Abstract S12A-03.

Briggs, R. W., et al. (2006), Deformation and slip along the Sunda megathrust in the great 2005 Nias-Simeulue earthquake, *Science*, *311*, 1897–1901.

Briggs, R. W., K. Sieh, W. H. Amidon, J. Galetzka, D. Prayudi, I. Suprihanto, N. Sastra, B. Suwargadi, D. Natawidjaja, and T. G. Farr (2008), Persistent elastic behavior above a megathrust rupture patch: Nias island, West Sumatra, *J. Geophys. Res.*, *113*, B12406, doi:10.1029/2008JB005684.

Cheng, H., R. L. Edwards, J. Hoff, C. D. Gallup, D. A. Richards, and Y. Asmerom (2000), The half-lives of uranium-234 and thorium-230, *Chem. Geol.*, *169*, 17–33.

Chlieh, M., J.-P. Avouac, K. Sieh, D. Natawidjaja, and J. Galetzka (2008), Heterogeneous coupling of the Sumatran megathrust constrained by geodetic and paleogeodetic measurements, *J. Geophys. Res.*, *113*, B05305, doi:10.1029/2007JB004981.

Clark, K. J., et al. (2013), Deriving a long paleoseismic record from a shallow-water Holocene basin next to the Alpine Fault, New Zealand, *Geol. Soc. Am. Bull.*, *125*, 811–832.

DeMets, C., R. G. Gordon, and D. F. Argus (2010), Geologically current plate motions, *Geophys. J. Int.*, *181*, 1–80.

Edwards, R. L., F. W. Taylor, and G. J. Wasserburg (1988), Dating earthquakes with high-precision thorium-230 ages of very young corals, *Earth Planet. Sci. Lett.*, *90*(4), 371–381.

Feng, L., E. M. Hill, P. Banerjee, I. Hermawan, L. L. H. Tsang, D. H. Natawidjaja, B. W. Suwargadi, and K. Sieh (2015), A unified GPS-based earthquake catalog for the Sumatran plate boundary between 2002 and 2013, *J. Geophys. Res. Solid Earth*, *120*, 3566–3598, doi:10.1002/2014JB011661.

Goldfinger, C., Y. Ikeda, R. S. Yeats, and J. Ren (2013), Superquakes and supercycles, *Seismol. Res. Lett.*, *84*(1), 24–32.

Harris, R., and J. Major (2016), Waves of destruction in the East Indies: The Wichmann catalogue of earthquakes and tsunami in the Indonesian region from 1538 to 1877, in *Geohazards in Indonesia: Earth Science for Disaster Risk Reduction*, *Geol. Soc. Spec. Publ.*, vol. 441, edited by P. R. Cummins and I. Meilano.

Hayes, G. P., D. J. Wald, and R. L. Johnson (2012), Slab1.0: A three-dimensional model of global subduction zone geometries, *J. Geophys. Res.*, *117*, B01302, doi:10.1029/2011JB008524.

Hill, E. M., et al. (2012), The 2010 M_w 7.8 Mentawai earthquake: Very shallow source of a rare tsunami earthquake determined from tsunami field survey and near-field GPS data, *J. Geophys. Res.*, *117*, B06402, doi:10.1029/2012JB009159.

Horton, B. P., P. L. Gibbard, G. M. Milne, R. J. Morley, C. Purintavaragul, and J. M. Stargardt (2005), Holocene sea levels and palaeoenvironments, Malay-Thai Peninsula, southeast Asia, *Holocene*, *15*(8), 1199–1213.

Jaffey, A. H., K. F. Flynn, L. E. Glendenin, W. C. Bentley, and A. M. Essling (1971), Precision measurements of half-lives and specific activities of ^{235}U and ^{238}U, *Phys. Rev. C*, *4*, 1889–1906.

Konca, A. O., et al. (2008), Partial rupture of a locked patch of the Sumatra megathrust during the 2007 earthquake sequence, *Nature*, *456*, 631–635.

Kositsky, A. P., and J.-P. Avouac (2010), Inverting geodetic time series with a principal component analysis-based inversion method, *J. Geophys. Res.*, *115*, B03401, doi:10.1029/2009JB006535.

Ludwig, K. R. (2003), Mathematical–statistical treatment of data and errors for ^{230}Th/U geochronology, *Rev. Mineral. Geochem.*, *52*(1), 631–656.

Ludwig, K. R., and D. M. Titterington (1994), Calculation of ^{230}Th/U isochrons, ages, and errors, *Geochim. Cosmochim. Acta*, *58*(22), 5031–5042.

Meltzner, A. J., K. Sieh, H.-W. Chiang, C.-C. Shen, B. W. Suwargadi, D. H. Natawidjaja, B. E. Philibosian, R. W. Briggs, and J. Galetzka (2010), Coral evidence for earthquake recurrence and an A.D. 1390–1455 cluster at the south end of the 2004 Aceh-Andaman rupture, *J. Geophys. Res.*, *115*, B10402, doi:10.1029/2010JB007499.

Meltzner, A. J., K. Sieh, H.-W. Chiang, C.-C. Shen, B. W. Suwargadi, D. H. Natawidjaja, B. Philibosian, and R. W. Briggs (2012), Persistent termini of 2004- and 2005-like ruptures of the Sunda megathrust, *J. Geophys. Res.*, *117*, B04405, doi:10.1029/2011JB008888.

Meltzner, A. J., et al. (2015), Time-varying interseismic strain rates and similar seismic ruptures on the Nias–Simeulue patch of the Sunda megathrust, *Quat. Sci. Rev.*, *122*, 258–281.

Natawidjaja, D. H., K. Sieh, S. N. Ward, H. Cheng, R. L. Edwards, J. Galetzka, and B. W. Suwargadi (2004), Paleogeodetic records of seismic and aseismic subduction from central Sumatran microatolls, Indonesia, *J. Geophys. Res.*, *109*, B04306, doi:10.1029/2003JB002398.

Natawidjaja, D. H., K. Sieh, M. Chlieh, J. Galetzka, B. W. Suwargadi, H. Cheng, R. L. Edwards, J.-P. Avouac, and S. N. Ward (2006), Source parameters of the great Sumatran megathrust earthquakes of 1797 and 1833 inferred from coral microatolls, *J. Geophys. Res.*, *111*, B06403, doi:10.1029/2005JB004025.

Natawidjaja, D. H., K. Sieh, J. Galetzka, B. W. Suwargadi, H. Cheng, R. L. Edwards, and M. Chlieh (2007), Interseismic deformation above the Sunda Megathrust recorded in coral microatolls of the Mentawai Islands, West Sumatra, *J. Geophys. Res.*, *112*, B02404, doi:10.1029/2006JB004450.

Newcomb, K. R., and W. R. McCann (1987), Seismic history and seismotectonics of the Sunda Arc, *J. Geophys. Res.*, *92*(B1), 421–439, doi:10.1029/JB092iB01p00421.

Perfettini, H., and J.-P. Avouac (2014), The seismic cycle in the area of the 2011 M_w9.0 Tohoku-Oki earthquake, *J. Geophys. Res. Solid Earth*, *119*, 4469–4515, doi:10.1002/2013JB010697.

Philibosian, B., K. Sieh, D. H. Natawidjaja, H.-W. Chiang, C.-C. Shen, B. W. Suwargadi, E. M. Hill, and R. L. Edwards (2012), An ancient shallow slip event on the Mentawai segment of the Sunda megathrust, Sumatra, *J. Geophys. Res.*, *117*, B05401, doi:10.1029/02011JB009075.

Philibosian, B., K. Sieh, J.-P. Avouac, D. H. Natawidjaja, H.-W. Chiang, C.-C. Wu, H. Perfettini, C.-C. Shen, M. R. Daryono, and B. W. Suwargadi (2014), Rupture and variable coupling behavior of the Mentawai segment of the Sunda megathrust during the supercycle culmination of 1797 to 1833, *J. Geophys. Res. Solid Earth*, *119*, 7258–7287, doi:10.1002/2014JB011200.

Reid, A. (2015), History and seismology in the Ring of Fire: Punctuating the Indonesian past, in *Environment, Trade and Society in Southeast Asia: A Longue Durée Perspective*, edited by D. Henley and H. S. Nordholt, pp. 62–77, Brill, Leiden, Netherlands.

Reid, A. (2016), Two hitherto unknown Indonesian tsunamis of the seventeenth century: Probabilities and context, *J. Southeast Asian Stud.*, *47*(1), 88–108.

Saji, N. H., B. N. Goswami, P. N. Vinayachandran, and T. Yamagata (1999), A dipole mode in the tropical Indian Ocean, *Nature*, *401*, 360–363.

Salman, R., E. M. Hill, S. Barbot, L. Feng, P. Banerjee, I. Hermawan, D. H. Natawidjaja, B. W. Suwargadi, and K. Sieh (2014), The 2008 Mw 7.2 North Pagai earthquake sequence and its relationship to ruptured and unruptured parts of the Mentawai patch, Abstract S41C-4498 presented at 2014 Fall Meeting, AGU, San Francisco, Calif.

Shen, C.-C., R. L. Edwards, H. Cheng, J. A. Dorale, R. B. Thomas, S. B. Moran, S. E. Weinstein, and H. N. Edmonds (2002), Uranium and thorium isotopic and concentration measurements by magnetic sector inductively coupled plasma mass spectrometry, *Chem. Geol.*, *185*, 165–178.

Shen, C.-C., et al. (2008), Variation of initial $^{230}Th/^{232}Th$ and limits of high precision U-Th dating of shallow-water corals, *Geochim. Cosmochim. Acta*, *72*(17), 4201–4223.

Shen, C.-C., et al. (2012), High-precision and high-resolution carbonate ^{230}Th dating by MC-ICP-MS with SEM protocols, *Geochim. Cosmochim. Acta*, *99*, 71–86.

Sieh, K., D. H. Natawidjaja, A. J. Meltzner, C.-C. Shen, H. Cheng, K.-S. Li, B. W. Suwargadi, J. Galetzka, B. Philibosian, and R. L. Edwards (2008), Earthquake supercycles inferred from sea-level changes recorded in the corals of west Sumatra, *Science*, *322*, 1674–1678.

Taylor, F. W., C. Frohlich, J. Lecolle, and M. R. Strecker (1987), Analysis of partially emerged corals and reef terraces in the central Vanuatu Arc; comparison of contemporary coseismic and nonseismic with Quaternary vertical movements, *J. Geophys. Res.*, *92*(B6), 4905–4933, doi:10.1029/JB092iB06p04905.

Zachariasen, J. (1998), Paleoseismology and paleogeodesy of the Sumatran subduction zone: A study of vertical deformation using coral microatolls PhD thesis, 418 pp., Calif. Inst. of Technol., Pasadena, Calif.

Zachariasen, J., K. Sieh, F. W. Taylor, R. L. Edwards, and W. S. Hantoro (1999), Submergence and uplift associated with the giant 1833 Sumatran subduction earthquake: Evidence from coral microatolls, *J. Geophys. Res.*, *104*(B1), 895–919, doi:10.1029/1998JB900050.

Zachariasen, J., K. Sieh, F. W. Taylor, and W. S. Hantoro (2000), Modern vertical deformation above the Sumatran subduction zone: Paleogeodetic insights from coral microatolls, *Bull. Seismol. Soc. Am.*, *90*(4), 897–913.